PEOPLE'S DEMOCRATIC REPUBLIC OF ALGERIA
MINISTRY OF HIGHER EDUCATION AND SCIENTIFIC RESEARCH
UNIVERSITY MOHAMED BOUDIAF OF M'SILA

FIELD: material science
SECTOR: Physics
OPTION: Medical physics

FACULTY OF SCIENCES
DEPARTMENT of PHYSICS
N°: PH/MED/08/2024

Thesis presented for obtaining the Professional Master's degree

Presented by: **LOUKRIZ TOUFIK**

Titled:

Design and Optimization of a Solar-Driven Autoclave System for Enhancing Sterilization Efficiency in Low-Resource Environment

Supported before the jury composed of:

SALMI Mohamed	Prof	UNIVERSITY MOHAMED BOUDIAF OF M'SILA	President
MAHDI Khaled	MCA	UNIVERSITY MOHAMED BOUDIAF OF M'SILA	Reviewer
BOUNAB Sabrina	MCA	UNIVERSITY MOHAMED BOUDIAF OF M'SILA	Examiner

Academic year: 2023 /2024

Acknowledgements

Praise be to Almighty God, who has given me faith, courage, and patience to carry out this work.

I would like to express my deep gratitude to my supervisor, Dr. Mahdi Khaled from the University Mohamed Boudiaf of M'Sila, for the confidence he has placed in me through his constant support, guidance, modesty, advice, and constructive remarks which greatly contributed to the successful progress of this work.

I also want to thank everyone who has helped me improve my work and who provided remarks that assisted me in perfecting this manuscript.

I extend my heartfelt thanks to my parents, my brothers, my sisters, and my entire family for their encouragement and prayers that enabled me to complete this modest project. I am deeply grateful for the confidence they have placed in me.

Finally, I express my gratitude to all those who have contributed in any way to the development of this work.

O Allah, send your blessings upon Your noble messenger, his family, and companions, and bless us in our lives.

Abstract

Developing countries face challenges in providing effective medical equipment sterilization methods due to resource and energy shortages. This thesis explores the integration of solar technology into autoclave design to improve sterilization efficiency in these regions. The research involves developing a mathematical model for a solar-powered autoclave system that meets required sterilization standards. Experiments have shown that the system can produce saturated steam and reach temperatures exceeding 121°C within 20 to 30 minutes, ensuring effective sterilization. The study highlights the importance of using renewable energy as a sustainable and efficient alternative to conventional energy sources in resource-limited settings.

Key words: *Solar technology, Autoclave design, Sterilization Efficiency, Medical Equipment, Developing Countries, Renewable Energy, Mathematical Model, Effective Sterilization.*

Résumé

Les pays en développement rencontrent des défis pour fournir des méthodes de stérilisation efficaces des équipements médicaux en raison du manque de ressources et d'énergie. Cette thèse examine l'intégration de la technologie solaire dans la conception des autoclaves pour améliorer l'efficacité de la stérilisation dans ces régions. La recherche comprend le développement d'un modèle mathématique pour concevoir un système d'autoclave alimenté par l'énergie solaire, répondant aux normes de stérilisation requises. Les expériences ont démontré que le système peut produire de la vapeur saturée et atteindre des températures supérieures à 121°C en 20 à 30 minutes, garantissant une stérilisation efficace. L'étude souligne l'importance de l'utilisation des énergies renouvelables comme alternative durable et efficace face à la pénurie d'énergie conventionnelle dans les pays en développement.

Mots clés :*Technologie solaire, Conception d'autoclave, Efficacité de la stérilisation, Équipements médicaux, Pays en développement, Énergie renouvelable, Modèle mathématique, Stérilisation efficac.*

Sources of Images

for Copyright purposes

Figure 1.1 from https://ilabot.blogspot.com/search/label/autoclave

Figure 1.2 from https://ilabot.blogspot.com/search/label/autoclave

Figure 1.3 from https://microbenotes.com/autoclave/

Figure 1.4 from https://www.iarjournals.com/upload/354252.pdf

Figure 1.5 from https://www.iarjournals.com/upload/354252.pdf

Figure 1.6 from https://statimusa.com/2022/09/the-history-of-the-autoclave/

Figure 1.7 from https://papers.ssrn.com/sol3/papers.cfm?abstract_id=3340320

Figure 2.1 from https://www.researchgate.net/publication/273177551_Development_and_construction_of_a_conical_solar_concentrator

Figure 2.2 from https://www.sciencedirect.com/science/article/pii/S1110016821002490

Figure 3.1 to 4.19 from https://linkinghub.elsevier.com/retrieve/pii/S2666818124000457

Contents

List of Figures

List of Tables

List of Abbreviations

HAIs : Health Care-Associated Infections
IPC : Infection Prevention and Control
PSI : Pounds per Square Inch
kW : Kilowatt
°C : Celsius
TSP : Central Receiver Towers
LFCs : Linear Fresnel Collectors
PTCs : Parabolic Trough Collectors
CDC : Centers for Disease Control and Prevention
$Q_{\mathbf{conv}}$: Heat transfer rate due to convection
$h_{\mathbf{lat}}$: Convective heat transfer coefficient for the lateral surface
$A_{\mathbf{lat}}$: Lateral surface area
$T_{\mathbf{lat}}$: Temperature of the lateral surface
$T_{\mathbf{env}}$: Ambient temperature
$h_{\mathbf{upp}}$: Convective heat transfer coefficient for the upper surface
$A_{\mathbf{upp}}$: Upper surface area
$T_{\mathbf{upp}}$: Temperature of the upper surface
$\lambda_{\mathbf{aut}}$: Thermal conductivity of the autoclave
D : External diameter of the autoclave
$\rho_{\mathbf{air}}$: Volumetric mass of air
$\mu_{\mathbf{air}}$: Dynamic viscosity of air
$N_{\mathbf{ulat}}$: Nusselt number of the autoclave lateral surface

Gr	: Grashof number
Pr	: Prandtl number
D^*	: Dimensions of the side of a square whose area is equal to the surface
$\varepsilon_{\mathbf{lat}}$	: Emissivity of the lateral surface of the autoclave
$\varepsilon_{\mathbf{ref}}$	: Emissivity of the conical surface of the concentrator/reflector
$\varepsilon_{\mathbf{upp}}$	: Emissivity of the upper surface of the autoclave
$J_{\mathbf{lat}}$	: Radiosity of the lateral surface
$J_{\mathbf{upp}}$	: Radiosity of the upper surface
$\varepsilon_{\mathbf{a}}$	: Emissivity of the atmospheric air
σ	: Stefan-Boltzmann constant
$m_{\mathbf{water}}$	: Mass of the water in the autoclave
$m_{\mathbf{aut}}$	: Mass of the autoclave
$c_{\mathbf{water}}$	: Specific heat capacity of water
$c_{\mathbf{aut}}$	: Specific heat capacity of the autoclave
$T_{\mathbf{aut}}(t)$	: Temperature of the autoclave as a function of time
IN	: Solar irradiance normal to the aperture area
$A_{\mathbf{ape}}$	: Aperture area of the solar concentrator
$\rho_{\mathbf{ref}}$	: Reflectivity of the concentrator
$\alpha_{\mathbf{lat}}$	: Absorptivity of the lateral surface
$F_{\mathbf{R}}$	: Heat removal factor
$\eta_{\mathbf{th}}$	: Thermal efficiency of the solar autoclave
$U_{\mathbf{L}}$	: Overall heat loss coefficient from the autoclave
$p_{\mathbf{sat}}$	: Saturated vapor pressure
p_0	: Boiling temperature of the water at a given pressure
M	: Molar mass of the water
$L_{\mathbf{v}}$	: Latent heat of vaporization of the substance
R	: Ideal gas constant

General introduction

Globally, hundreds of millions of people are affected every year by avoidable infections in health care (health care-associated infections, HAIs). The determinants of HAI are influenced by a complex combination of gaps in policies, infrastructure, organization and knowledge, defects in health-care workers' behavior, and patientrelated factors. Through knowledge, best practices and infrastructures improvement, infection prevention and control (IPC) aims to prevent harm due to HAI to patients and health workers. Sterilization and decontamination of instruments and medical devices play a very important role in the prevention of HAIs. Indeed, defective sterilization of surgical instruments and disinfection of reusable objects including endoscopic devices, respiratory care devices, and reusable hemodialysis devices still occur in many settings and lead to HAIs. In addition, in many low-resource settings inappropriate reuse of disposable medical devices is common practice and the procedures to clean and decontaminate these devices are inadequate and not standardized. The processes of sterilization and decontamination are complex, require specific infrastructure and equipment and involve several steps that need to be correct, from devices collection, receipt by the unit, processing, storage and distribution them throughout the facility. Of utmost importance are also quality control procedures to assess the correct functioning of the equipment.[1] Developing countries face significant challenges due to a lack of resources, hindering their efforts to improve living conditions for their citizens. Among the most prominent of these challenges are medical care and clean, reliable energy. As medical care advances, some communities often remain unable to afford modern technologies that can be life-saving. These advancements, which make medical care more efficient, usually require large amounts of energy. For example, a 76,000-square-foot American hospital consumes approximately $.3-4 per square foot annually. Due to the difficulty in providing the necessary energy in developing countries, many people suffer from infectious diseases due to the difficulty in sterilizing medical equipment. Of particular importance is that bacterial contamination resulting from non-sterilized medical equipment poses a significant problem for developing countries, leading to widespread infections and sometimes hospital closures. These contaminants cause gastrointestinal diseases that can range from severe diarrhea and colitis to death. These issues are not always targeted in

traditional sterilization standards, making their elimination difficult. One reason for the ineffectiveness of sterilization practices is the lack of energy sources, making proper sterilization a significant problem. Therefore, it is essential to seek cheap alternative energy options.

Renewable energy appears to be a clear solution to focus on, as non-renewable energy can be expensive, representing a particular concern for developing countries. Several reasons make it necessary for developing countries to focus on developing renewable energy :

- The availability of open spaces in many areas allows for the use of solar energy.
- Traditional energy sources are harmful to health and destroy environments.
- Solar panels are cheaper than other forms of renewable energy, making them ideal for supplying small households and villages in rural areas.

Fossil fuels produce pollution linked to serious health problems. For example, the World Bank estimates that 780 million women and children inhaling kerosene fumes are equivalent to inhaling smoke from two packs of cigarettes daily. In contrast, solar energy produces no fumes, leaves no waste, and is much cheaper than fossil fuels. With fossil fuels being non-renewable, the transition to renewable energy is very important, especially in the field of medical equipment sterilization.

To address this issue, an affordable autoclave that uses solar energy to effectively sterilize medical equipment can be designed and developed. To achieve this goal, it is necessary to understand two main points : First, the biology of the targeted bacteria must be studied, which is not the focus of this project. Second, it is essential to understand how all the elements of the solar autoclave work and develop them according to sterilization needs. In this project, we focused on developing and improving every part of the solar autoclave to ensure it achieves sterilization efficiency similar to that provided by traditional autoclaves. We also aimed to design an easy-to-maintain device that is effective in destroying pathogenic microorganisms.[2]

In this study, we present a mathematical model applied to the concentration of solar energy. This system is designed to prepare steam to meet the sterilization needs of medical instruments. A conical concentrator coupled to an autoclave in cylindrical form is placed on the conical reflector axis. We present a mathematical model explaining the thermal behavior of water in a medical autoclave. The model's validation was well done with the literature results. Our results indicate that the system produces saturated steam and takes 20 to 30 minutes, depending on climatic conditions and autoclave dimensions. This is sufficient time to reach a temperature of more than 121°C, where no organism

reproduces after being kept in an autoclave at 126°C for 6 minutes or at 121°C for at least 20 minutes. The simulation results encourage us to optimize the concentrator device to obtain a useful solar sterilizer, using the theoretical model as a safe guide to achieve this. Before describing the design and testing methodology, it is essential to address the challenges related to the sterilization process to ensure the effectiveness of the designed system.[3]

0.1 Problem Statement

1. **Inadequate Sterilization Practices :** Many healthcare facilities, particularly in developing countries, face challenges with ineffective sterilization of surgical instruments and reusable devices, leading to persistent HAIs.
2. **Resource Constraints :** Developing countries struggle with insufficient resources for proper sterilization and decontamination due to inadequate infrastructure and unreliable energy sources. This impacts their ability to maintain effective sterilization practices.
3. **Energy Limitations :** Traditional sterilization processes often require substantial amounts of energy, which is a significant barrier in regions with unreliable or costly energy supplies. The lack of energy hinders effective sterilization procedures.
4. **Need for Alternative Energy Sources :** Reliance on non-renewable energy sources is costly and harmful to the environment. Solar energy offers a viable alternative that can address both energy and cost issues related to sterilization.
5. **Development of Affordable Solar Sterilizers :** To address these challenges, the research proposes designing an affordable solar autoclave that uses solar energy to achieve effective sterilization of medical equipment. This involves developing a system capable of producing steam efficiently to meet sterilization needs and ensuring that the device is cost-effective and easy to maintain.

To address these challenges, we implemented a comprehensive work plan. The study focuses on developing and optimizing a solar sterilization system, incorporating a mathematical model to enhance solar energy concentration and ensure effective sterilization. The primary objective is to design a system capable of producing saturated steam efficiently and within a practical timeframe, while addressing various issues related to the sterilization process. We relied on the following research plan :

0.2 Research Plan

The research presented in this thesis is structured to provide a thorough understanding of the components and functionality of the solar autoclave. The work plan is organized as follows :

- **Chapter One : Traditional Autoclave Technology**
  This chapter offers a detailed exploration of traditional autoclave technology, laying the foundation for understanding the evolution and need for alternative sterilization methods.
- **Chapter Two : Solar Collectors**
  This chapter delves into solar collectors, examining their role in harnessing solar energy and their integration into the autoclave system.
- **Chapter Three : Numerical Study and Optimization of the Conical Autoclave Receiver**
  This chapter presents a detailed numerical investigation and optimization of the conical autoclave receiver. It delves into the intricacies of design parameters and evaluates performance metrics with a focus on enhancing system efficacy. By integrating insights from Chapter One and Chapter Two, this chapter offers a comprehensive and cohesive analysis, addressing key aspects of system design and operational performance. The discussion extends to the refinement of design strategies and the optimization of functional parameters, contributing to a robust understanding of the autoclave's operational characteristics and its potential for improved performance.
- **Chapter Four : Results and Impact**
  This chapter presents the results of the research, demonstrating the efficacy of the solar autoclave and its potential impact on healthcare practices.
- **General Conclusion**
  In conclusion, this thesis integrates the analysis of traditional autoclave technology with advancements in solar energy utilization to propose an innovative approach to sterilization. The findings emphasize the feasibility and benefits of the solar autoclave system, potentially influencing future healthcare sterilization practices.

Chapitre 1

General Description of Medical Autoclaves

1.1 Introduction to Medical Autoclaves

1.1.1 Definition and Purpose

Autoclave is a device that sterilizes laboratory instruments, glassware and medical equipment by using highly pressurized saturated steam to effectively kill microorganisms. An Autoclave is a sealed vessel that operate at high temperature and pressure in order to kill microorganisms and spores. Biological hazards are also rendered inactive by an autoclave machine. Autoclaves provide a physical method for disinfection and sterilization. They work with a combination of steam, pressure and time. Autoclaves are used to sterilize tools and equipment in medical, dental and laboratory environments by treatment with high temperature steam. Prior to the use of autoclaves, sterilization was frequently performed using boiling water at 100C, an insufficient treatment as many bacteria and microorganisms survive temperatures up to 120C.The steam temperature of the autoclave must therefore exceed 120C to reach adequate sterilization (Vårdhandboken, 2011). According to present regulations, a temperature of 134C must be upheld for at least 3 minutes inside the sterilization chamber. The pressure inside the sterilization chamber is increased in order to obtain dry saturated steam with the temperature suitable for sterilization. Fossil fuel remains a major source of power for such equipment in the absence of hydro generated electricity.[4]

1.1.2 Types of Autoclaves :

There are many different aspects that can be used as a basis for the categorization of the different types of autoclaves, and some of these aspects may overlap with each other. In most cases, steam sterilizers can be differentiated by :

- Function
- Class
- Size (capacity)

1.1.2.1 Different Types of Autoclaves Categorized by Function : All autoclaves use high-temperature and high-pressure steam to sterilize medical equipment and waste. Their function indicates how they should be loaded, and how they force in the steam in their chamber to sterilize the instruments inside.

Vertical Autoclaves : These types of autoclaves are loaded by opening their top lid. They are especially suited for laboratory use or in smaller clinics with cramped spaces. As such, they also have a smaller capacity chamber.

FIGURE 1.1 : Vertical Autoclaves

Horizontal Autoclaves : Front-loading steam sterilizers with a larger capacity chamber. When available space is not an issue, and you need to treat many loads a day, this one is exceptional for reducing the strain on medical staff.

FIGURE 1.2 : Horizontal Autoclaves

Gravity Displacement Autoclaves : One of the most common types of autoclave that relies on using dense steam to force out the air from the machine's chamber. They are suitable for the treatment of basic loads like flat surgical tools and certain types of biohazardous waste but are not as versatile as prevacuum autoclaves.

Pre-vacuum (Prevac) Autoclaves : This type of autoclave uses a vacuum pump to remove all the air from the autoclave's chamber, allowing for better steam penetration and the sterilization of more materials and complex loads such as medical textile products, porous loads, larger pieces of equipment, and even objects made from high-density polyethylene like the syringes of sharps and pipette tips.

1.1.2.2 Different Types of Autoclaves Categorized by Class : A more clear-cut way of categorizing the different types of autoclave machines. A steam sterilizer's class indicates how versatile it is : in other words, it shows what kind of loads can be treated with it.

Class N Autoclaves : These are essentially simple, gravity displacement autoclaves that only remove a certain portion of the air inside the machine's chamber. Designed for the treatment of simpler loads like flat medical tools.

Class S Autoclaves : Another type of gravity displacement autoclave that uses a wall of dense steam, but by repeating the process three times, it can actually extract all the air from the chamber, and as such, it can already treat bagged instruments and porous loads. Still less versatile and not as fast as a class B autoclave though.

Class B Autoclaves : Premium pre-vacuum autoclaves that can sterilize the most materials and are also much faster at doing so by removing all the air from their chamber with a powerful vacuum pump. Some models make the best out of modern technology and operate with a completely automated process : this ease-of-use and effectiveness make them very attractive for all kinds of medical facilities.

FIGURE 1.3 : some type of autoclave

1.1.2.3 Different Types of Autoclaves Categorized by Size (Capacity) : Here is a categorization that is pretty straightforward, but it certainly does not make it less important to consider. Autoclave size is also a key factor that needs to be taken into account : the right choice here depends on the amount of waste your facility needs to treat each day, as well as the amount of available space you have.

Large Steam Sterilizers : The capacity of these types of autoclaves usually ranges between 110 to 880 liters. Ideal for large medical facilities like hospitals that generate a notable amount of waste each day and need to use a lot of medical tools and equipment to treat patients.

Medium-sized Steam Sterilizers : The capacity of these types of autoclaves usually ranges between 75 to 200 liters. An excellent choice for dental and other clinics, biotechnological applications, or for operating theaters in hospitals.

Small (Benchtop) Steam Sterilizers : The capacity of these types of autoclaves usually moves around 25 liters. These compact steam sterilizers are perfectly suited for smaller facilities with limited available space, and who do not need to sterilize as many medical tools each day.

[5]

1.2 Design and Components

1.2.1 Design

The autoclave consists of a double-walled cylinder. The outer wall has a diameter of 300 mm, while the inner cylinder has a diameter of 260 mm. This double-walled design helps to keep the heat inside and provides strong support. The inner cylinder has small holes that allow steam to enter when the water boils, ensuring that steam can reach all parts of the items inside for effective sterilization.

Figure 1.4 shows the sterilization cylinder and the inner container. The sterilization cylinder is where items are placed for sterilization. It is made of stainless steel, which can handle high temperatures and does not react with other materials. The inner container is used to hold the items being sterilized and is also made of durable materials. The figure highlights the structure of the cylinder, showing the double walls and the perforations in the inner cylinder that allow steam to circulate evenly. [4]

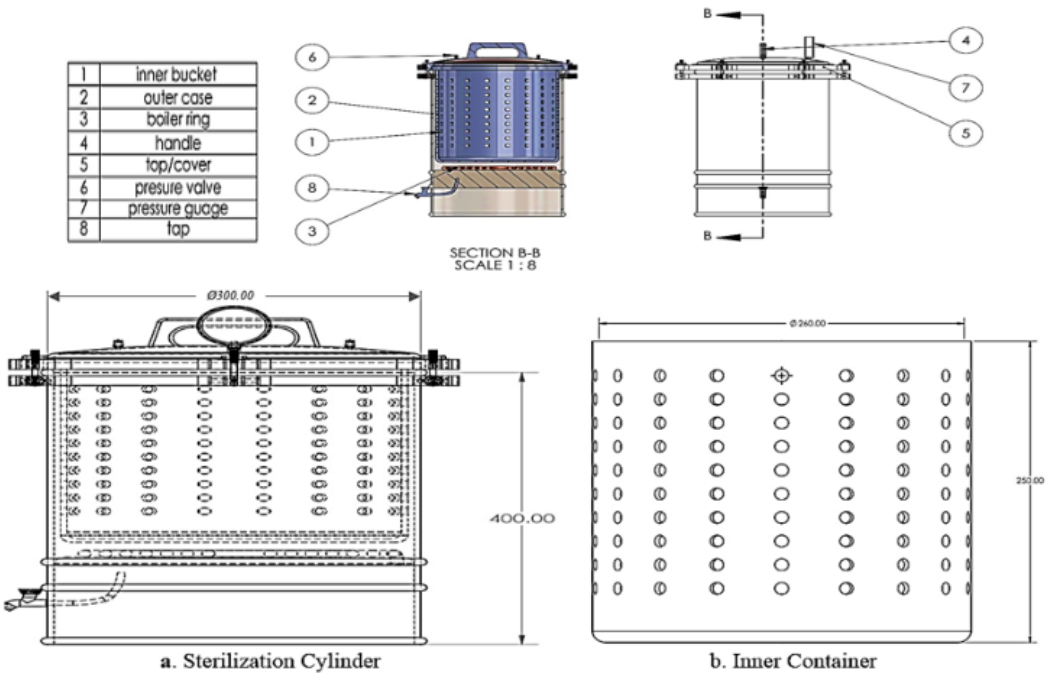

FIGURE 1.4 : Sterilization cylinder and inner container

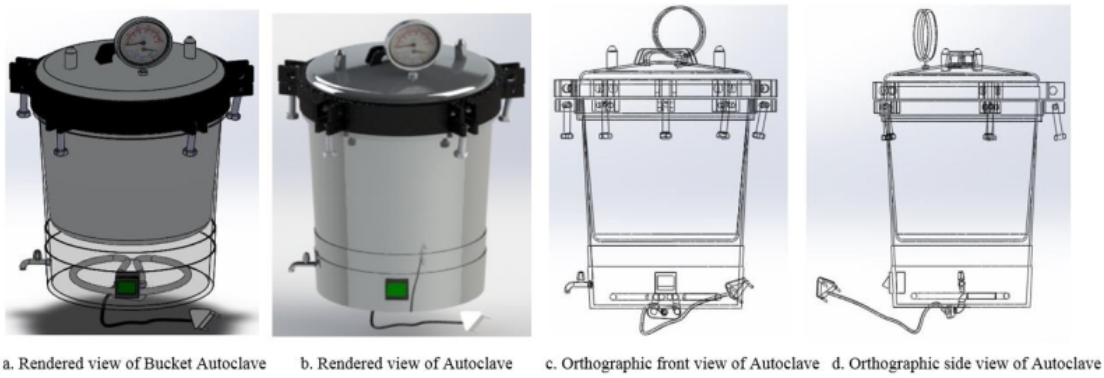

FIGURE 1.5 : Computer aided designs of autoclave

1.2.2 Components

1. Chamber : The place where the materials to be sterilized are placed. It is made from stainless steel alloy due to its high durability at high temperatures and its non-reactivity with other materials (such as salts). The chamber has a thickness of about 1 inch, which resists high pressure and provides complete protection for the user. It is connected with several parts such as a safety valve, pressure meter, heater, and thermostat. Inside the chamber, there is a basket used to elevate the autoclaved materials away from the heater and water.

2. Pressure Meter : The pressure is measured by a mechanical gauge in units of pounds per square inch (PSI). Gauge pressure is the difference between the pressure in the chamber and the atmospheric pressure.

3. Thermostat/Thermometer : A particularly flexible control that allows ON/OFF control of the sterilizer. It has one output controlled by a microprocessor according to the value programmed for the parameters. The display during the basic function shows the variable measured by the probe, and when programming, it indicates the value chosen for the control parameters. The parameters are shown and set using the four keys on the front panel. This type of thermostat ensures the temperature remains stable, providing a safe range for the materials to be autoclaved and a more secure system for the user. Types of thermostats include :

1. *Mechanical Thermostat :* The mechanical thermostat operates by the thermal expansion factor, which varies between metals. It uses a method where two metal laminas, one made from copper and the other from iron, are joined together. Since copper has a higher thermal expansion factor than iron, the flexion of the duple occurs, limiting the electrical current to maintain a fixed temperature.

4. Safety Valve : A system that uses mechanical principles with a spring to push a lever that closes a pipe from which steam exits. This part ensures a safety system for the user in case the thermostat fails or is damaged.

5. Timer : A mechanical device used to estimate the time cycle needed for autoclaving a material. It consists of various pulleys, levers, and springs that work together to give a specific signal indicating the end of the adjusted time period. This timer type is used because it turns off all parts (thermometer, heater, etc.) of the device after the adjusted time period, making it easy to use.

6. Heater : The electrical heating system produces heat by raising the temperature through the passage of electric current through a conductor with high resistance. The heater is an ingot of iron and carbon coated by two layers : an inner layer of china and an outer layer of metal, usually the same as the inner heater metal. It is a water heater that operates without water and is covered by an insulated material to protect the device from any hazard. It is made from stainless steel and has a circular shape.

7. Indicator Lamps : The device contains indicator lamps : green for indicating the heater is working, red for the power supply, and yellow for indicating the process is finished. The red lamp is connected parallel to the power switch, the green lamp is connected parallel to the heater, and the yellow lamp is connected parallel to the buzzer to indicate

the end of the autoclaving operation.

8. Switches : The device contains an ON/OFF switch for power, consisting of mechanical parts that can handle high current (ranging between 0-15 A). It also includes a multi-ON switch with two operations : the first operation turns on the heater and thermostat to achieve the desired chamber temperature (e.g., 121°C and 15 PSI), while the second operation turns on the heater, thermostat, and timer to operate the device for a specific time period with the initial chamber specifications.[6]

1.3 The History of the Autoclave

1.3.1 Evolution of Autoclave Technology

The necessity of autoclaves is intrinsically linked to the broader concept of sterilization. The practice of sterilization dates back to approximately 3000 BCE, when the Egyptians employed pitch and aromatic substances for embalming bodies with remarkable skill. During the period between 130 and 220 CE, the Greek physician Galen gained medical authority through his findings, including the boiling of instruments used to treat wounded soldiers. However, progress in sterilization stagnated after around 900 CE as diseases became rampant and towns were ravaged by plagues. Significant advancements did not occur until the Renaissance, which marked the beginning of microorganism detection and the development of superheated steam machines.

1.3.1.1 Innovations of the Renaissance : The Renaissance introduced two crucial inventions relevant to autoclaves : the pressure cooker and the microscope. In 1680, French physicist Denis Papin invented a pressure cooking device known as the “Digester,” which created a tight seal between the pot and lid. This device trapped hot air, causing it to expand and increase the boiling point of water inside, effectively cooking food with superheated steam. In 1683, Antoni van Leeuwenhoek, a Dutch linen draper and scientist, developed the first true microscope, achieving magnification up to 270x and pioneering the study of microorganisms.

1.3.1.2 Advancements in the Nineteenth Century : In 1876, Charles Chamberland, a collaborator and pupil of Louis Pasteur, invented the first practical autoclave for steam sterilization, building upon Denis Papin’s “Digester.” Chamberland’s autoclave marked a significant milestone in the field of sterilization, following Pasteur’s invention of pasteurization in 1862.

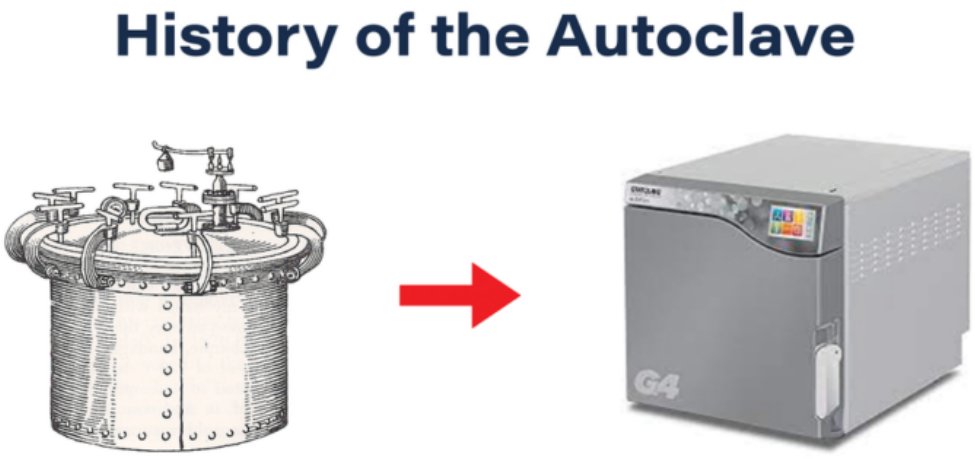

FIGURE 1.6 : The development of the autoclave device over time.

1.3.2 Prominent Autoclave Manufacturers

1. **Tuttnauer**

   Tuttnauer commenced its autoclave manufacturing operations in 1925, initially serving the British Army. By 1987, the company expanded its operations to the United States, establishing itself as a prominent authority in the field of laboratory autoclaves. Tuttnauer's products are utilized across a range of sectors, including hospitals, veterinary clinics, and prestigious universities. Notably, the company operates the world's largest autoclave manufacturing facility, encompassing over 325,000 square feet.

2. **Scican/Coltene**

   Scican/Coltene entered the autoclave market in 1989 with the introduction of the Statim Cassette Autoclave. This pioneering device drastically reduced sterilization times from the conventional 45 minutes to just six minutes. The need for faster sterilization solutions gained prominence following a significant 1992 incident, in which the transmission of the AIDS virus via an infected dental instrument highlighted the critical importance of rapid sterilization in dental practices.

3. **Midmark**

   Founded in 1915 in Minster, Ohio, Midmark originally operated as the Cummings Machine Company, specializing in the manufacture of concrete mixers. The company's foray into the medical sector began in the 1950s. Following the acquisition of the Reeves Pulley Company in 1920, Midmark diversified into locomotive production. By the 1960s, under the leadership of Carl F. Eiting and subsequently James A. Eiting, the company refocused on the medical market. Midmark's growth conti-

nued through acquisitions, including Ritter and Knight Manufacturing, and it now maintains a global presence with offices in France, India, the United Kingdom, and Italy. This strategic evolution has established Midmark as a well-recognized name in the medical industry.

4. **Enbio**
   Enbio, a Swiss manufacturing company with over 30 years of expertise in biotechnology and industrial hydroponics, produces all its products in-house. The company employs a team of structural engineers, software programmers, and industrial designers. Enbio has developed a broad global network extending across Europe, the Middle East, and the United States, with an annual turnover exceeding 200 million euros. Its expansion into the U.S. market has cemented its position as a significant player in the autoclave industry.

These manufacturers have been instrumental in the advancement of autoclave technology, driving progress in sterilization practices across various industries.[7]

1.4 Operating Principle of an Autoclave

Steam sterilization, commonly achieved through autoclave technology, involves the use of high-temperature steam to sterilize heat-resistant objects. This process typically operates at temperatures ranging from 121°C to 140°C and pressures between 16 and 35 psi. As one of the most reliable sterilization methods, steam sterilization effectively eliminates microorganisms by causing irreversible coagulation and denaturation of their enzymes and structural proteins. The presence of moisture is crucial, as it significantly impacts the temperature required for protein coagulation and microorganism destruction.

An autoclave functions by exposing clean medical devices to a controlled environment of steam, temperature, and pressure. Key parameters for effective sterilization include steam, temperature, pressure, and time. Saturated steam and entrained water are used to achieve the necessary temperatures, with pressure playing a critical role in reaching the high temperatures needed to eradicate microorganisms. For standard sterilization, wrapped medical devices must be exposed to 121°C for at least 30 minutes or to 132°C for 4 minutes in a prevacuum sterilizer. However, specific requirements can vary depending on the type of medical device.

Autoclaves are generally categorized into two types : gravity displacement and high-speed prevacuum sterilizers. Gravity displacement autoclaves are frequently used in laboratories for processing media, medical waste, water, pharmaceutical products, and nonporous devices. These autoclaves may require longer penetration times due to incomplete air

removal, as illustrated by the decontamination of microbiological waste, which takes at least 45 minutes at 121°C due to reduced steam permeation and heating efficiency.

High-speed prevacuum sterilizers, on the other hand, are equipped with a vacuum pump or ejector that removes air from the sterilizing chamber before introducing steam. This feature allows for nearly instantaneous steam penetration into porous loads. The effectiveness of air removal is verified using tests such as the Bowie-Dick test, which uses folded 100% cotton surgical towels to detect any residual air and ensure adequate air removal.

Steam sterilization utilizes a pulsing process, combining steam and pressure pulses above atmospheric pressure to rapidly expel air. This method ensures effective sterilization even if minor air leaks occur, as the steam remains above atmospheric pressure throughout the process. Typical conditions for sterilization involve temperatures between 132°C and 135°C, with exposure times of 3 to 4 minutes for porous loads and instruments. The sterilization process is monitored using mechanical, chemical, and biological indicators, with effectiveness verified through printouts or graphical representations of temperature, time, and pressure [8].

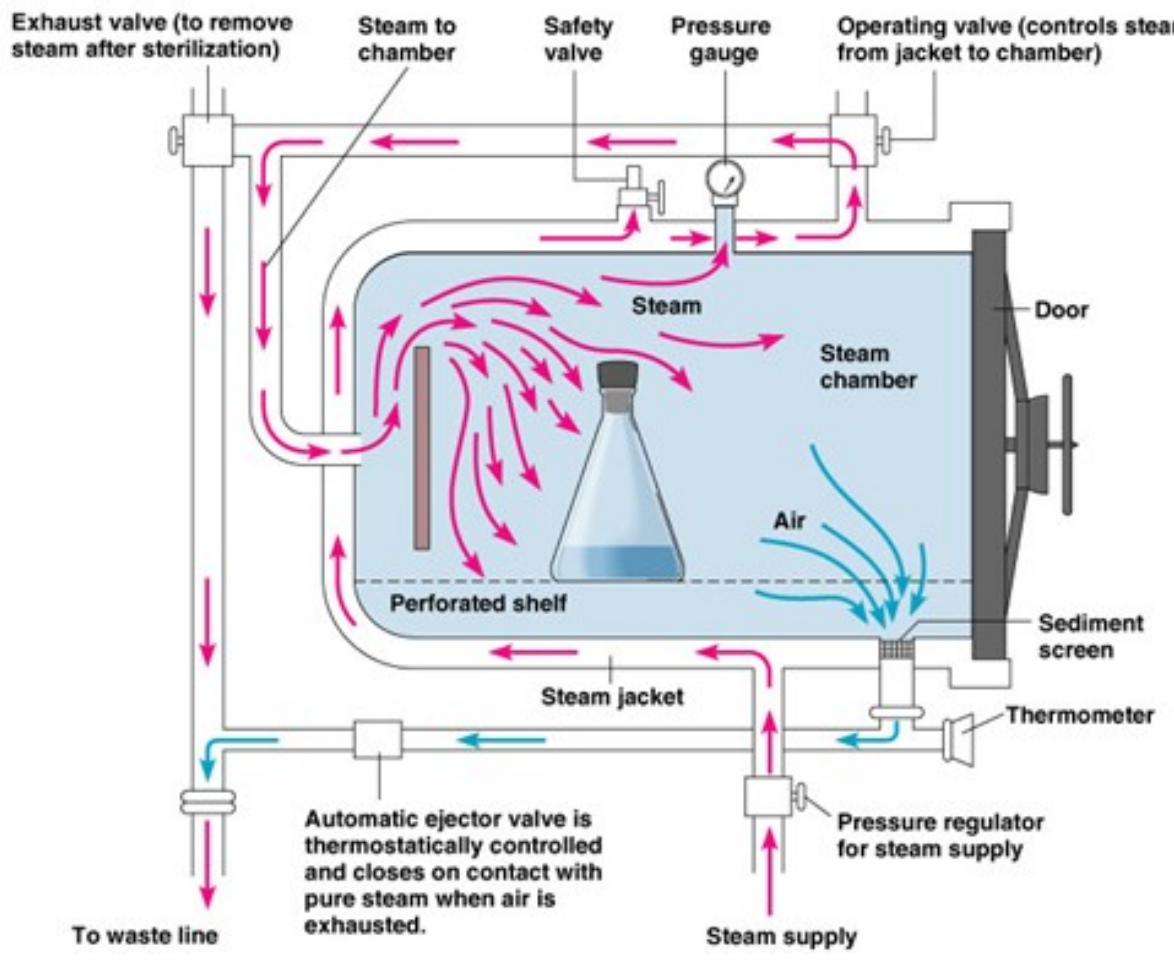

FIGURE 1.7 : Operating Principle of an Autoclave

Chapitre 2

Solar Concentration

2.1 Introduction to Solar Concentration

In recent years, solar energy has garnered substantial attention due to its diverse potential applications, driven primarily by the ongoing search for alternative energy sources in response to the depletion and rising costs of fossil fuels. As one of the most abundant and widely accessible renewable resources, solar energy is available in both direct and indirect forms. The sun emits an enormous amount of energy, approximately 3.8×10^{23} kW., and Earth, located about 150 million kilometers away, receives around 60% of this radiation, equating to approximately 1.08×10^{14} kW. advantage over other energy sources—its cleanliness and lack of environmental pollution.

Historically, fossil fuels have dominated energy supplies due to their lower costs and ease of use, with minimal concern for environmental impacts until recent times. In contrast, modern solar energy technologies require high-grade energy to achieve compact plant sizes and efficient power generation with short payback periods. Although directly available solar energy is considered low-grade, concentrated solar energy technology emerges as a compelling alternative for more efficient energy production. In this context, solar concentrators assume a pivotal role in enhancing the efficiency of solar energy utilization and broadening its applications, particularly in the field of medical sterilization. Advanced solar concentrators address the technical and commercial challenges associated with conventional concentrated solar energy systems but also offer a promising solution for improving the performance and cost-effectiveness of medical sterilization systems. Consequently, they contribute significantly to more efficient and sustainable practices within this critical sector.[9]

2.2 Overview of Solar Concentrators and Their Types

2.2.1 Theoretical Background

Solar concentrators are sophisticated devices designed to enhance the intensity of solar radiation by focusing it onto a smaller area. These systems employ optical components, such as mirrors or lenses, to concentrate sunlight for applications that require elevated temperatures, including power generation, refrigeration, and space heating. By channeling solar energy onto a reduced focal point, concentrators significantly increase the energy density compared to natural sunlight.

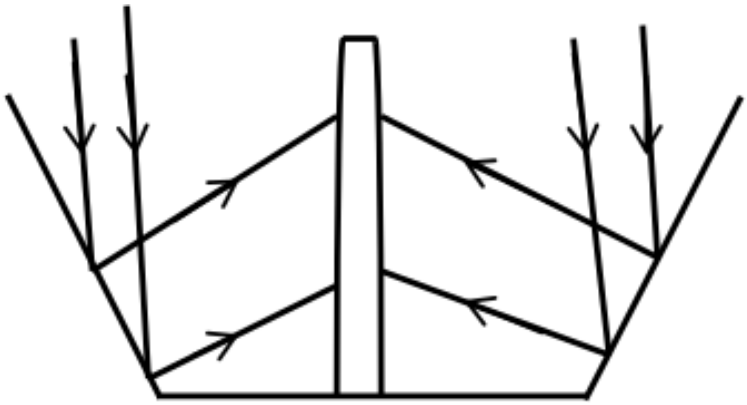

FIGURE 2.1 : Reflection By A Conical Surface

2.2.2 Key Components of Solar Concentrators

The key components of solar concentrators include :

- **Reflecting or Refracting Surfaces :** These surfaces capture and focus sunlight onto the absorber.
- **Absorbing Surfaces and Fluids :** The absorber captures the concentrated solar energy and transfers it to a fluid, such as air, water, or oil.
- **Tracking Systems :** To maintain optimal alignment with the sun, concentrators use tracking systems that adjust the position of the collector.
- **Storage Systems :** The collected heat can be stored in thermal energy tanks for later use.[10]

2.3 Types of Solar Collectors

Solar collectors are categorized into two main types :

2.3.1 Stationary Solar Collectors

Stationary solar collectors are permanently fixed in position and do not track the sun.

2.3.2 Sun Tracking Solar Collectors

Sun tracking solar collectors focus on reducing heat losses by concentrating large amounts of solar radiation onto a small collection area. This is achieved using advanced optical devices that focus solar light onto an energy receiver. This technique produces temperatures significantly higher than those achievable with flat-plate collectors, thereby enhancing system efficiency.

2.3.2.1 Parabolic Dish Collectors : These collectors use a dish-shaped mirror to gather and direct sunlight onto a central receiver. This design achieves high concentration ratios, resulting in elevated temperatures. It is primarily used in applications requiring very high temperatures.

2.3.2.2 Parabolic Trough Collectors (PTCs) : These collectors feature a cylindrical mirror that concentrates sunlight onto a receiver tube extending along the mirror's focal line. This type of collector is widely used in commercial solar power plants due to its high efficiency and extensive practical experience.

2.3.2.3 Linear Fresnel Collectors (LFCs) : This type consists of linear mirrors that focus sunlight onto a receiver positioned along the line of mirrors. This configuration provides a cost-effective solution compared to parabolic dishes or troughs.

2.3.2.4 Central Receiver Towers (TSP) : This arrangement involves a central tower surrounded by a field of heliostats, which are mirrors with two-axis tracking systems. These heliostats concentrate solar energy onto a receiver located at the top of the tower. This technology is employed in large-scale energy generation projects due to its capability to produce substantial amounts of power.[9]

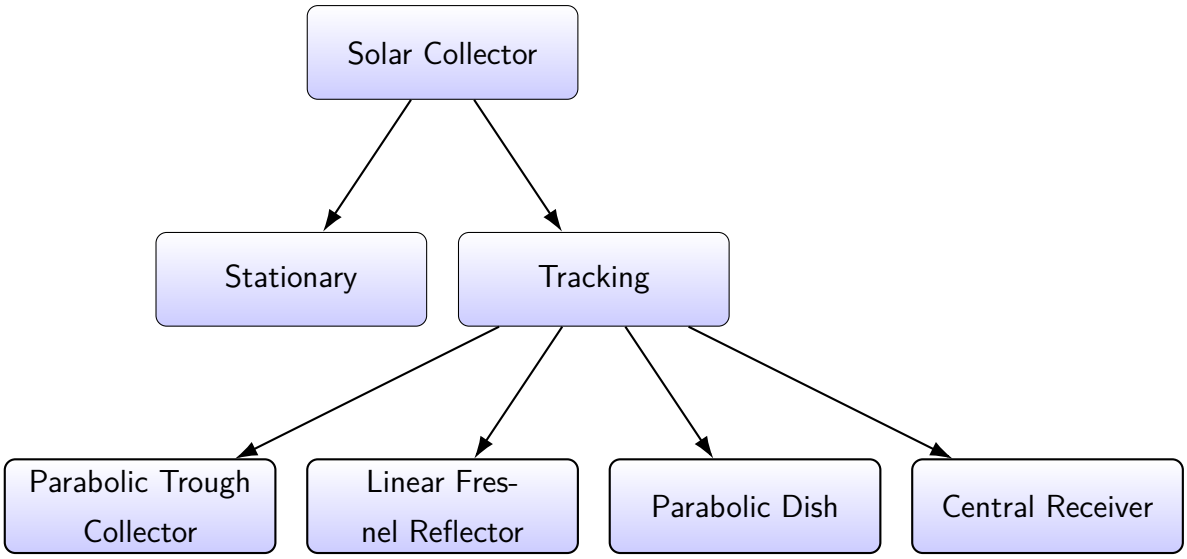

Figure 2.1.1 : Types of Solar Collectors.

2.4 Advanced Technologies for Solar Concentrator-Based Autoclaves

Solar concentrator-based autoclaves leverage advanced solar thermal technologies to enhance the efficiency of medical sterilization processes. These systems can be classified based on the type of solar concentrator technology employed and the method of thermal energy transfer from the solar collectors to the autoclave. The primary systems utilized are :

2.4.1 Solar Parabolic Dish Collector Powered Autoclave

This system resembles a large satellite dish with mirrored reflectors that concentrate solar radiation at the focal point, where the autoclave is installed. The autoclave, typically painted black, converts solar energy into thermal energy, heating the fluid to the required sterilization conditions. This technology often utilizes a two-axis tracking system for continuous sun tracking but can also employ a manual orientation mechanism to reduce costs. The heat transfer rate is high because the autoclave is maintained at the focal point of the dish.

2.4.2 Parabolic Trough Collector Powered Autoclave

This system concentrates solar radiation on an absorber tube through which the heat transfer fluid circulates. The steam generated in the absorber is directed to the autoclave, facilitating the sterilization process. This system also requires a sun tracking device.

2.4.3 Fresnel Collector Powered Autoclave

This collector uses horizontally aligned reflector segments that follow the sun using a tracking device. The absorber heats the working fluid, which is then converted to steam for the autoclave. An alternative Fresnel technology uses a Fresnel lens with concentric rings to focus solar radiation on the autoclave, reducing costs by eliminating the need for an absorber and using a lighter, more durable plastic lens.

2.4.4 Evacuated Tube Collector Powered Autoclave

Constructed from a series of glass tubes connected to header pipes, this collector absorbs solar radiation in the outer shell of each tube. The generated heat turns the working fluid into steam, which is stored in the autoclave for sterilization.

2.4.5 Flat Plate Collector Powered Autoclave

Similar to the evacuated tube collector, this technology uses blackened metal absorbers welded onto tubes through which the working fluid flows. The tubes are installed in an insulated box covered by glass. Both technologies must be mounted at a tilt to allow condensed working fluid to return for reheating. These collectors do not concentrate solar rays and must be optimally designed to reach the minimum sterilization temperature of 121°C.

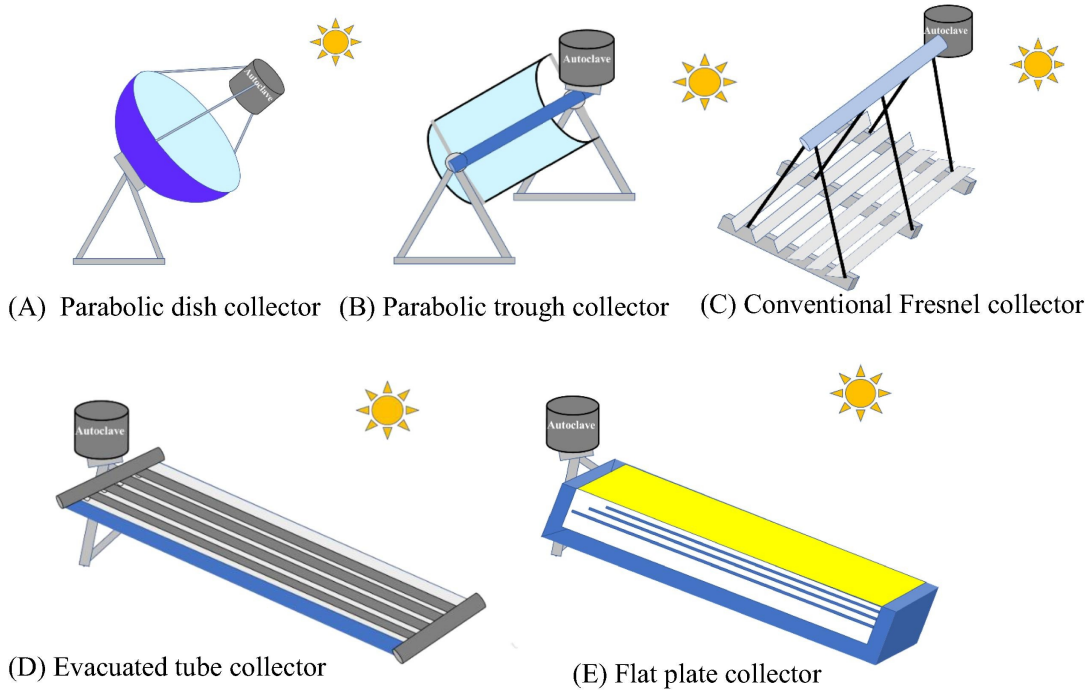

FIGURE 2.2 : Conventional solar thermal collectors powered autoclave

2.5 Heat Transfer Methods

Regarding heat transfer methods, solar autoclaves can be categorized as direct or indirect :

2.5.1 Direct Solar Autoclaves

These autoclaves do not use a working fluid. Solar radiation is redirected by the collector to an absorber device at the bottom of the autoclave, converting radiative energy into thermal energy, which heats the sterilization fluid inside the autoclave through conduction.

2.5.2 Indirect Solar Autoclaves

In these systems, solar energy is first converted into thermal energy by a collector with an absorber. The heat is then transferred to the autoclave using a thermal fluid or working fluid. This category can be further divided into :

2.5.2.1 Single Working Fluid Systems : The same fluid acts as both the solar and sterilization fluid.

2.5.2.2 Dual Working Fluid Systems : An intermediate heat exchanger transfers heat between the solar collector and the autoclave. Various thermal fluids, including oil and nanofluids, can be used, though care must be taken to avoid negative environmental or medical impacts.

2.6 Review of Historical Advances in Solar Concentrator Technologies for Medical-Surgical Autoclave Sterilization

This section provides a comprehensive review of the historical advancements in solar concentrator technologies that have been applied to the sterilization of medical and surgical equipment. It traces the evolution of various techniques and innovations that have contributed to the development of solar-powered autoclaves.

The review encompasses the different methods utilized to generate and manage the working fluids necessary for effective sterilization. Additionally, it explores the evolution of solar radiation concentration techniques, including early and modern implementations of Fresnel lenses, reflective mirrors, and parabolic dishes. By examining these historical developments, this section highlights the progress made in optimizing solar concentrator technologies and their role in enhancing the efficiency and effectiveness of medical-surgical sterilization processes.

Bahadori, Mehdi N. (1976)[11] : In his 1976 study published in Solar Energy, Bahadori presents the design and testing of a portable solar autoclave aimed at sterilizing medical instruments. The autoclave, designed for handling up to 7.5 kg of equipment, features a dual-cylinder structure. The inner cylinder contains the instruments, while the outer cylinder collects solar energy. This energy is concentrated by segmented mirrors arranged on the inner surface of a truncated cone. Water fills the space between the cylinders, and the unit is oriented towards the sun to maximize solar exposure. This design demonstrates an innovative approach to utilizing solar energy for effective medical sterilization.

Tyroller, M. (2006)[12] : Tyroller (2006) presents the development and installation of a solar steam sterilizer for rural hospitals in a conference paper. The sterilizer operates using a 10 m^2 Scheffler Reflector, which stores thermal heat in a 230 kg iron block functioning as a steam generator. The system runs hybrid, allowing the use of an electrical boiler during periods of low solar radiation. This setup provides a sustainable and effective solution for sterilizing medical equipment in rural healthcare settings.

Schuler, Douglas A., Kaseman, Tremayne, and Boubour, Jean (2012)[13] : In their 2012 study published in The American Journal of Tropical Medicine and Hygiene, Schuler, Kaseman, and Boubour evaluate the effectiveness of a solar-thermal powered autoclave designed for wet sterilization of medical instruments in off-grid environments. The

authors conducted twenty-seven trials using a non-electric autoclave with simulated medical instrument bundles and biological test agents. The results indicated that the autoclave consistently reached temperatures exceeding 121 °C for 30 minutes in all trials, demonstrated effective steam sterilization through indicator tape reactions, and eliminated microbial agents, meeting the CDC's standards for wet sterilization.

Trabia, Sarah (2012)[2] : Trabia's 2012 Master's thesis, submitted to the University of Nevada, Las Vegas, focuses on designing and testing a solar autoclave intended for use in developing countries. The thesis addresses the challenges of limited energy access and aims to create a cost-effective, non-electric autoclave capable of sterilizing medical equipment against a range of bacteria, including Biosafety Level 2 pathogens. Despite the design's potential, the study reports that the autoclave did not achieve the required temperature and pressure levels. The thesis includes a discussion on the experimental errors and offers recommendations for future research to develop a fully functional solar autoclave.

Dravid, (2012)[14] : In their April 2012 article published in Journal of Hospital Infection, Dravid and colleagues explore the development of a portable solar-powered autoclave in India. The study highlights the use of the Prince-40 Concentrator, which proved effective for autoclaving culture media and treating biomedical waste in a small laboratory setting. The technology not only provides a sustainable alternative to conventional energy sources but also offers significant cost savings, potentially saving up to Rs. 15,000 annually in electricity or Rs. 37,500 in LPG costs. This solar autoclave technology is particularly beneficial for rural health centers experiencing frequent power outages or lacking reliable electricity.

Neumann,(2013)[15] : In their 2013 study published in Proceedings of the National Academy of Sciences, Neumann and colleagues introduce a compact solar autoclave designed to address the sterilization needs in resource-limited settings. This autoclave utilizes broadband light-harvesting nanoparticles to generate high-temperature steam. The study demonstrates that the autoclave effectively uses solar energy for sanitation, verified through standard Geobacillus stearothermophilus-based biological indicators. The system provides a viable solution for medical and dental practices in developing regions where conventional sterilization methods are scarce.

Lawrence,(2013)[16] : Lawrence and colleagues present a final report in 2013 from the Department of Mechanical Engineering at Northern Arizona University on the design of a solar autoclave for rural areas. The report explores the potential of solar autoclaves as a solution for sterilizing medical equipment in regions lacking reliable electricity. The solar

autoclave design aims to achieve steam sterilization by pressurizing water to produce temperatures exceeding 121 °C. Although the prototype approached the target temperature and pressure, heat loss during testing impacted performance. The report outlines design considerations and recommendations for improving efficiency and reliability in future iterations.

Chandler, David L. (2013)[17] : In a February 2013 article, Chandler reports on the development of the SolarClave, a solar-powered autoclave project by MIT's Little Devices group. The SolarClave aims to replace traditional kerosene or electric sterilizers in remote clinics with a cost-effective, locally repairable alternative. The project, initiated in Nicaragua, has adapted the design based on user feedback to enhance functionality and safety. By eliminating the need for fuel or electricity, the SolarClave offers a sustainable solution for sterilizing medical tools in underserved areas, demonstrating a practical application of solar technology in improving health care access.

Sadhana, (2014)[18] : In their 2014 article in the International Journal of Emerging Technology and Advanced Engineering, Sadhana, Prasad, and Satyanand investigate the design of a cylindrical parabolic concentrator for sterilization purposes. The study focuses on the challenge of ensuring high levels of sterility for medical equipment, particularly in areas lacking advanced technology. The authors propose a solar autoclave that uses a cylindrical parabolic concentrator to generate steam required for effective sterilization. By harnessing solar radiation, this method offers a practical and cost-effective solution for sterilizing medical instruments, making it especially useful in remote or underdeveloped regions where conventional electric autoclaves are not feasible.

Buxbaum, Ryan (2015)[19] : In his 2015 capstone project report for the Duke University Certificate in Energy and Environment, Buxbaum addresses the challenge of sterilizing medical equipment in rural clinics without reliable electricity. The report outlines a design for a non-electric autoclave that uses a curved solar reflector to concentrate sunlight onto a pressure cooker, thus generating the necessary pressurized steam for sterilization. This approach aims to replace expensive electric autoclaves and mitigate the need for reliable grid infrastructure. The study includes an analysis of environmental and social impacts, as well as a business plan for implementing the solar autoclave in rural communities. Despite initial challenges in reaching certified sterilization temperatures due to variations in solar irradiance and testing conditions, the project demonstrates a promising solution for sustainable medical equipment sterilization.

Sharma, (2017)[20] : In their 2017 article published in the Indian Journal of Science and Technology, Sharma et al. present the design and development of a cost-effective solar

autoclave. The study focuses on creating a solar panel and autoclave system for steam sterilization of medical equipment and disposal of hospital waste. The authors designed a solar parabolic trough to generate steam and a vessel capable of operating as an autoclave, using low-cost materials. The autoclave achieved a maximum temperature of 132°C and pressure of 15 PSI, demonstrating effective sterilization. The overall cost of the materials was approximately Rs.30,000, making it a feasible solution for remote areas. The design can be further refined by optimizing the vessel size and safety valve modifications.

Thomas, (2017)[21] : Thomas et al. (2017) propose a combined autoclave and water purification system utilizing solar energy in their article published in the International Journal for Innovative Research in Science and Technology. The system aims to address water scarcity and sterilization challenges by using renewable solar energy to purify contaminated water. The integration of these functions into a single system provides a dual solution to both water purification and medical sterilization, offering an innovative approach to resource management in areas with limited access to electricity.

Haileslasie, (2019)[22] : Haileslasie, Abrha, and Minas (2019) discuss the performance analysis of a solar autoclave designed for rural health centers in their study published in the Momona Ethiopian Journal of Science. The research evaluates a solar thermal-based autoclave, comparing its performance with standard sterilization techniques. The autoclave achieved temperatures of approximately 145°C, maintained for over 20 minutes, meeting sterilization standards. The field trials demonstrated the system's potential to improve healthcare delivery in off-grid health centers, providing a practical solution to sterilize medical equipment and reduce health risks in rural settings.

Birhanu, H. (2018)[23] : In their 2018 article published in the International Journal of Advanced Research in Engineering and Technology, Birhanu and Kahsay present the design, manufacturing, and testing of a solar autoclave for rural clinics. The solar autoclave uses a parabolic dish concentrator and a pressure cooker to generate steam for sterilizing surgical instruments. Tests showed that the autoclave could continuously achieve a steam temperature of 121°C and pressure of 2 bars for 30 minutes. Modifications to the relief valve increased the maximum temperature to 128°C and pressure to 2.6 bars, demonstrating the potential of solar autoclaves to replace electrical autoclaves in areas without reliable electricity.

Wang, X. (2019)[24] : In their 2019 paper published in Progress in Natural Science : Materials International, Wang et al. present a solar steam generator that produces high-temperature steam at ambient pressure. The generator uses a coiled copper tube (CCT) coated with black superhydrophobic copper oxide to enhance solar absorption and prevent

condensation. The system achieved steam temperatures exceeding 100°C under 1-sun illumination and up to 250°C under 10-sun illumination. Successful sterilization experiments validated its potential for medical sterilization and other high-temperature steam applications.

Zhao, L., Bhatia, B. (2020)[25] : In an article on Physics World, Zhao and Bhatia (2020) describe a solar-powered device developed by MIT and IIT Bombay researchers for sterilizing medical equipment. The device uses a portable solar energy collector and a transparent silica aerogel to generate high-temperature, high-pressure steam. Field tests in Mumbai validated the device's sterilization efficacy using standard autoclave indicator tape. The system offers a low-cost, reliable solution for sterilizing medical tools in remote areas without dependable electricity.

Yadav, M. (2021)[26] : In the 2021 conference proceedings of the 7th International Conference on Advances in Energy Research, Yadav, Modi, and Kedare describe a solar autoclave designed for rural hospitals, utilizing aerogel as a transparent insulation material. The proposed autoclave uses a compound parabolic concentrator to focus sunlight and an aerogel layer to reduce thermal losses, eliminating the need for costly tracking systems. Experiments showed that the aerogel collector effectively generated saturated steam for sterilization, meeting the load requirements of nearby hospitals. This non-tracking design offers a cost-effective solution for sterilizing surgical instruments in areas with unreliable electricity.

Mahdi, K. (2024)[3] : In a 2024 article published in Partial Differential Equations in Applied Mathematics, Mahdi et al. present a mathematical model for a conical autoclave receiver designed to concentrate solar energy for medical sterilization. The system includes a conical concentrator coupled with a cylindrical autoclave. The model describes the thermal behavior of water in the autoclave, showing that it can produce saturated steam within 20 to 30 minutes, depending on climatic conditions and autoclave dimensions. The study demonstrates the system's capability to reach temperatures of 121°C for sterilization, with potential optimization guided by the theoretical model to enhance its effectiveness as a solar sterilizer.

Chapitre 3

Modeling an Autoclave Operating with Concentrated Solar Radiation

3.1 Introduction

This chapter presents a detailed analysis based on the article titled *Numerical Study and Optimization of a Conical Autoclave Receiver*[3]. The article introduces an innovative mathematical model designed for the concentration of solar energy, with the specific aim of generating steam for the sterilization of medical instruments. The system integrates a conical concentrator with a cylindrical autoclave, positioned strategically along the axis of the reflector to enhance energy capture and steam production.

This research is grounded in a comprehensive thermodynamic study, capturing the transient behavior of the system through an energy balance equation, leading to a partial differential equation (PDE) governing the temperature evolution within the autoclave and the water contained therein. Solutions to this PDE, obtained using the fourth-order Runge-Kutta numerical method, provide critical insights into the time-dependent temperature profiles essential for effective sterilization.

Simulation results indicate that the system is capable of producing saturated steam within 20 to 30 minutes, a duration influenced by climatic conditions and autoclave dimensions. The model's predictions align with experimental data, demonstrating that the autoclave can achieve and maintain temperatures exceeding 121°C, ensuring the destruction of microorganisms when exposed to 126°C for 6 minutes or 121°C for at least 20 minutes.

To validate the proposed model, extensive simulation tests were performed. These simulations utilized a precisely designed system incorporating a conical reflector, a cylindrical tube (the autoclave), and a pressure regulator. The reflector's tracking system was opti-

mized to maximize solar radiation capture, thereby enhancing overall system efficiency. The simulation results were rigorously compared with existing literature, revealing a high degree of agreement, underscoring the robustness of the theoretical model.

The study is organized as follows : initially, we apply the Brichambaut model to calculate direct solar radiation at the M'Sila site. This is followed by the development of a mathematical model to predict temperature evolution and saturated steam pressure within the autoclave. Subsequent sections discuss the performance of the designed system under various seasonal conditions, concluding with a comprehensive summary of the study's findings and their implications for future solar sterilization systems.

3.2 Design of the Conical Autoclave

The concentrator is designed with a precisely engineered conical shape, featuring an interior surface coated with a reflective material. This reflective coating is essential for enhancing the system's performance by maximizing the concentration of solar energy onto the target area. The conical concentrator is mounted on a sophisticated support system that includes two rotational axes, enabling the concentrator to track the sun's path throughout the day. This tracking capability ensures continuous alignment with the sun, optimizing the collection of solar energy.

The autoclave, a critical component of the system, is constructed from high-conductivity copper (360 $W/°C \cdot m^2$), selected for its superior thermal properties. This choice of material ensures efficient heat absorption and transfer, crucial for effective sterilization. The autoclave is designed as a cylindrical tube with external diameters varying from 5 to 10 cm and a constant length of 50 cm. It includes an aperture for water filling, with capacity adjustments based on the selected diameter, and is equipped with a safety valve to ensure leak-proof operation.

To further enhance the system's efficiency, the autoclave is coated with a thin layer of black paint. This coating reduces the reflection of concentrated solar rays from the conical reflector, thereby increasing the amount of absorbed solar energy. The autoclave is aligned along the central axis of the conical concentrator to maximize energy absorption. The cone of the concentrator is engineered with a half-angle of 45°, optimizing the concentration of solar radiation. A model illustrating this setup is depicted in Fig.3.1.

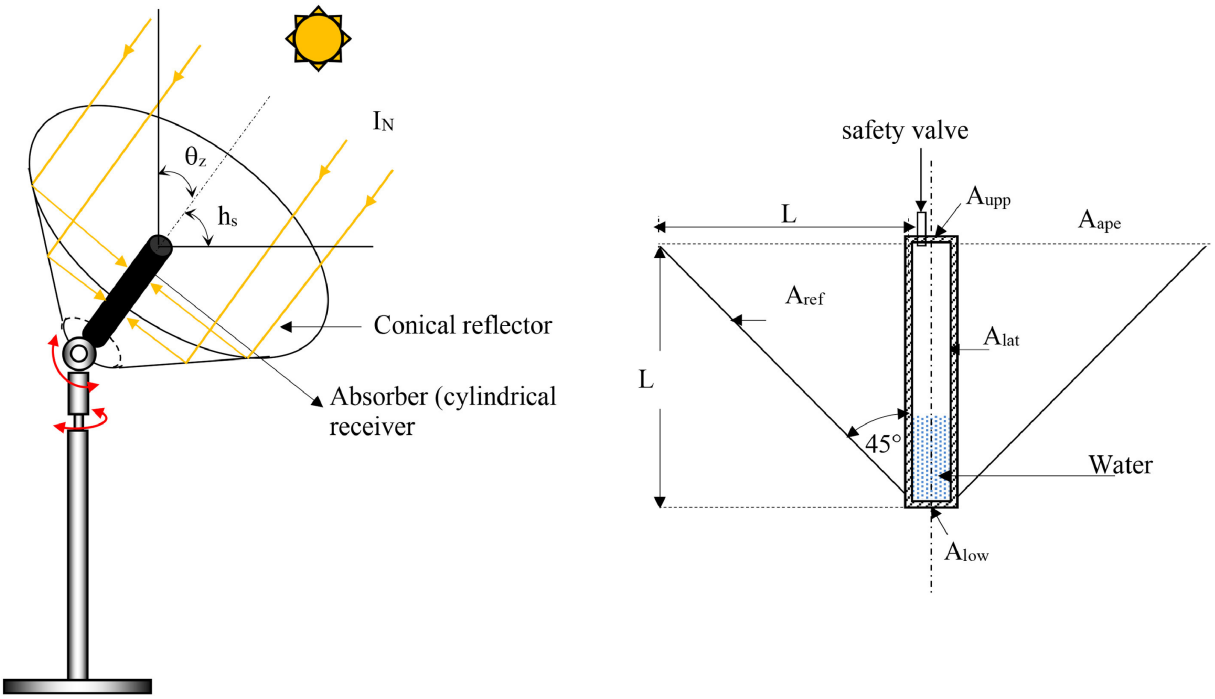

FIGURE 3.1 : Schematic of solar autoclave configuration.

Where :

- A_{ref} : Reflector surface of the conical concentrator
- A_{ape} : Aperture surface
- A_{lat} : Lateral surface of the autoclave
- A_{upp} : Upper surface of the autoclave
- A_{low} : Lower surface of the autoclave
- L : Length of the autoclave/cylinder and radius of the aperture reflector
- θ_z : Zenith angle
- h_s : Solar height

3.3 Mathematical model

The mathematical model is composed mainly of two parts ;

- **he first calculates the direct incident radiation using solar radiation models**
- **The second is based on calculating the temperature and heat transfer parameters by convection**

3.4 Calculation of Normal Direct Solar Radiation

3.4.1 Declination Angle (δ)

The solar autoclave was theoretically tested under M'Sila's climatic conditions on December 21 and June 21, with computations from 11 :00 a.m. to 01 :00 p.m. M'Sila, located at 340 m above sea level in central Algeria (latitude 35.71° N, longitude 4.54° E), has a continental climate characterized by the Brichaumbot model. Direct solar radiation, though attenuated, can penetrate the atmosphere, and its intensity is calculated using various methods. The declination value can be accurately obtained using the following formula.

$$\delta = 23.45^\circ \sin\left(\frac{360}{365}\left(284 + n_{\text{day}}\right)\right) \tag{3.1}$$

where n_{day} is the day of the year.

3.4.2 Hour Angle (ω)

The position of the sun in the sky gives us information about solar time ST, which is given by sundials. There is a simple relationship between solar time ST and the hour angle w, given by :.

$$\omega = (ST - 12) \times 15 \tag{3.2}$$

where ST is the solar time in hours.

3.4.3 The notion of average time (STM)

The notion of average time (STM), which varies by ±16 min about ST, is given by the following formula :

$$\mathrm{STM} = \mathrm{ST} - \mathrm{ET} \tag{3.3}$$

3.4.4 Equation of Time (ET)

The equation of time (ET) accounts for discrepancies between solar time and clock time due to the Earth's elliptical orbit and axial tilt. It is used to correct solar time to local mean time.

$$ET = 229.2\,(0.000075 + 0.001868\cos B - 0.032077\sin B - 0.014615\cos 2B - 0.04089\sin 2B) \tag{3.4}$$

where $B = \frac{360}{365}\,(n_{\mathrm{day}} - 81)$.

3.4.5 Solar Zenith Angle (θ_z)

The solar zenith angle (θ_z) is the angle between the sun and the vertical direction at a given location. It is essential for determining how much solar radiation reaches the Earth's surface.

$$\theta_z = \arccos\left(\cos(\mathrm{lat})\cos(\delta)\cos(\omega) + \sin(\mathrm{lat})\sin(\delta)\right) \tag{3.5}$$

3.4.6 Solar Elevation Angle (h_s)

The solar elevation angle (h_s) is the apparent angle of the sun above the horizon. It is crucial for calculating the intensity of solar radiation reaching the Earth's surface.

$$h_s = \arcsin\left(\cos(\mathrm{lat})\cos(\delta)\cos(\omega) + \sin(\mathrm{lat})\sin(\delta)\right) \tag{3.6}$$

3.4.7 Atmospheric Pressure ($P_{\mathbf{atm}}$)

Atmospheric pressure (P_{atm}) decreases with altitude. This pressure affects the amount of solar radiation reaching the Earth's surface.

$$P_{\text{atm}} = 101325 \left(1 - z \times 2.26 \times 10^{-5}\right)^{5.26} \tag{3.7}$$

where z is the altitude in meters.

3.4.8 Saturation Vapor Pressure ($P_{\mathbf{vs}}$)

The saturation vapor pressure (P_{vs}) represents the maximum pressure exerted by water vapor in the air at a given temperature. It is an important parameter in atmospheric science.

$$P_{\text{vs}} = 2.165 \left(1.098 + 0.01 T_{\text{env}}\right)^{8.02} \tag{3.8}$$

where T_{env} is the environmental temperature in °C.

3.4.9 Partial Pressure of Water Vapor (P_v)

The partial pressure of water vapor (P_v) is calculated from the saturation vapor pressure and the relative humidity. It affects the absorption of solar radiation by the atmosphere.

$$P_v = P_{\text{vs}} \times U \tag{3.9}$$

where U is the relative humidity.

3.4.10 Relative Optical Air Mass (m)

The relative optical air mass (m) quantifies the amount of atmosphere that solar radiation travels through, affecting its attenuation.

$$m = \frac{P_{\text{atm}}}{[101{,}325 \sin(h_s) + 151{,}98.75 \times (3.8{,}85 + h_s) - 1.25{,}3]} \tag{3.10}$$

3.4.11 Rayleigh Optical Thickness (E_R)

Rayleigh optical thickness (E_R) describes the attenuation of solar radiation due to Rayleigh scattering in the atmosphere.

$$E_R = \frac{1}{0.9m + 9.4} \tag{3.11}$$

3.4.12 Linke Turbidity Factor (T_L)

The Linke turbidity factor (T_L) represents the amount of dust and water vapor in the atmosphere affecting solar radiation.

$$T_L = 2.4 + 14.6d + 0.4\,(1 + 2d)\ln(P_v) \tag{3.12}$$

Where d is the coefficient of atmospheric disorder, taking the following values :

- $d = 0.02$ for a mountain location ;
- $d = 0.05$ for a rural location ;
- $d = 0.10$ for an urban location ;
- $d = 0.20$ for an industrial location (polluted atmosphere).

.

3.4.13 Extraterrestrial Radiation (G_{on})

Extraterrestrial radiation (G_{on}) is the solar radiation received at the top of the Earth's atmosphere.

$$G_{on} = G_{sc}\left(1 + 0.033\cos\left(\frac{360 n_{day}}{365}\right)\right) \tag{3.13}$$

where G_{sc} is the solar constant, approximately 1367 W/m^2.

3.4.14 The calculation of incident radiation :

$$I_N = G_{on} \times e^{-(E_R \times m \times T_L)} \tag{3.14}$$

3.4.15 Radiation Flux on the Autoclave's Lateral Surface as Depicted in Fig 3.1

$$Q_{aut} = I_N A_{ape} \rho_{ref} \alpha_{aut} \tag{3.15}$$

3.5 Concentration Ratio of the Cone Reflector

The concentration ratio C_R of a conical reflector is a measure of how effectively the reflector concentrates solar energy onto the autoclave relative to the area of the autoclave's side surface. It is defined as :

$$C_R = \frac{A_{\text{apr}}}{A_{\text{lat}}} \tag{3.16}$$

where A_{apr} is the area of the conical reflector and A_{lat} is the area of the autoclave's lateral surface. The analysis considers autoclave diameters D_{aut} of 0.025, 0.03, 0.035, 0.04, 0.045, and 0.05 meters, with a fixed reflector diameter D_{ref} of 1 meter.

3.6 Energy Balance of the Autoclave

The energy balance equation for the solar autoclave system equates the absorbed solar energy to the useful heat produced plus the thermal losses. The general energy balance equation is :

$$Q_{\text{aut}} = Q_{\text{use}} + Q_{\text{los}} \tag{3.17}$$

where :

- Q_{aut} is the energy absorbed by the autoclave,
- Q_{use} is the useful heat produced,
- Q_{los} represents the total thermal losses.

The energy absorbed by the autoclave system from the conical reflector is :

$$Q_{\text{aut}} = \eta_o Q_s \tag{3.18}$$

Knowing that :where η_o is the optical efficiency of the reflector

$$\eta_O = \rho_{\text{ref}} \alpha_{\text{lat}}$$

Where : Absorption coefficient, respectively, of the side and upper surface of the autoclave

$$\alpha_{\text{aut}} = \alpha_{\text{lat}} = \alpha_{\text{upp}}$$

and Q_s is the solar energy incident on the reflector :

$$Q_s = I_N A_{\text{ref}} \tag{3.19}$$

Here, I_N is the normal incident solar radiation and A_{ref} is the area of the reflector.

3.7 Useful Heat Produced

The useful heat produced can be calculated as follows from the energy balance of the autoclave. The absorbed solar energy by the autoclave, Q_{aut}, is separated into useful heat (Q_{use}) and thermal losses (Q_{los}). The absorbed power (Q_{abs}) is calculated from the solar power (Q_{s}) and the optical efficiency (η_O) :

$$\eta_O = \rho_{\text{ref}} \alpha_{\text{aut}}$$

Moreover, in steady state, thermal losses (Q_{los}) can be separated into three categories : heat losses by radiation (Q_{rad}), heat losses by internal convection (Q_{conv})

$$Q_{\text{los}} = Q_{\text{rad}} + Q_{\text{conv}} \tag{3.20}$$

3.8 Thermal Losses

Thermal losses are categorized into :

- **Internal convection thermal losse**
- **Radiation thermal losses**

3.8.1 Internal convection thermal losse

Convection heat losses occur due to heat transfer to the environment through convective processes :

$$Q_{\text{conv}} = h_{\text{lat}} A_{\text{lat}} \left(T_{\text{lat}} - T_{\text{env}}\right) + h_{\text{upp}} A_{\text{upp}} \left(T_{\text{upp}} - T_{\text{env}}\right) \quad (3.21)$$

where :

- h_{lat} is the convective heat transfer coefficient for the lateral surface,
- A_{lat} is the lateral surface area,
- T_{lat} is the temperature of the lateral surface,
- T_{env} is the ambient temperature,
- h_{upp} is the convective heat transfer coefficient for the upper surface,
- A_{upp} is the upper surface area,
- T_{upp} is the temperature of the upper surface.

The values of the heat transfer coefficients of the lateral surface h lat are highly dependent on the velocity of the wind blowing with respect to the cylinder. the heat transfer coefficient h_{lat} is given by :

$$h_{\text{lat}} = 0.174 \frac{\lambda_{\text{aut}}}{D} \left(\frac{\rho_{\text{air}} V_{\text{wind}} \cos h_s D}{\mu_{\text{air}}} \right)^{0.618} \quad (3.22)$$

where

- λ_{aut} : Thermal conductivity of the autoclave.
- D : External diameter of the autoclave.
- ρ_{air} : Volumetric mass of air.
- μ_{air} : Dynamic viscosity of air.

We can also calculate the Nusselt number using the following formula :

$$Nu_{\text{lat}} = \frac{h_{\text{lat}} D}{\lambda_{\text{aut}}} \quad (3.23)$$

and

$$Nu_{\text{lat}} = 0.174 \left(\frac{\rho_{\text{air}} V_{\text{wind}} \cosh_s D}{\mu_{\text{air}}} \right)^{0.618} \quad (3.24)$$

Where :

- Nu_{lat} : Nusselt number of the autoclave lateral surface.

The coefficient of the upper surface h_{lat}, when the wind speed is zero, is given by :

$$h_{\text{lat}} = \frac{k}{D^*} \left(Gr \times Pr \times \cosh_s\right)^{0.25} \tag{3.25}$$

with

$$Nu_{\text{lat}} = \left(Gr \times Pr \times \cosh_s\right)^{0.25} \tag{3.26}$$

where :

- Gr : Grashof number.
- Pr : Prandtl number.

and

$$D^* = \sqrt{\pi \frac{D^2}{4}} \tag{3.27}$$

D^* : Dimensions of the side of a square whose area is equal to the surface. We can find the value of the Grashof number using the relation

The Grashof number (Gr) and the Prandtl number (Pr) are defined as :

$$\text{Gr} = \frac{gy\Delta T L^3 \rho^2}{\mu^2} \tag{3.28}$$

and

$$\text{Pr} = \frac{\mu c_p}{k} \tag{3.29}$$

where $\Delta T = T_{\text{aut}} - T_{\text{ref}}$ is the temperature difference.

3.8.2 Radiation Heat Losses

Then radiation heat losses are given by

$$Q_{\text{rad-lat}} = \frac{A_{\text{lat}}\varepsilon_{\text{lat}}}{1-\varepsilon_{\text{lat}}}\left(\sigma T_{\text{lat}}^4 - J_{\text{lat}}\right) + \frac{A_{\text{upp}}\varepsilon_{\text{upp}}}{1-\varepsilon_{\text{upp}}}\left(\sigma T_{\text{upp}}^4 - J_{\text{upp}}\right) \tag{3.30}$$

Where the radiosities J_{lat} and J_{upp} are developed in the appendix and are given by :

$$J_{\text{lat}} = \varepsilon_1 \sigma T_{\text{lat}}^4 + (1-\varepsilon_{\text{lat}})\left(\varepsilon_{\text{ref}} F_{\text{lat-ref}} + \varepsilon_{\text{a}} F_{\text{lat-ape}}\right)\sigma T_{\text{env}}^4 \tag{3.31}$$

$$J_{\text{upp}} = \varepsilon_2 \sigma T_{\text{upp}}^4 + (1-\varepsilon_{\text{upp}})\left(\varepsilon_{\text{g}} F_{\text{upp-g}} \sigma T_{\text{g}}^4 + \varepsilon_{\text{a}} F_{\text{upp-s}} \sigma T_{\text{env}}^4\right) \tag{3.32}$$

where :

- ε_{lat} : emissivity of the lateral surface of the autoclave.
- ε_{ref} : emissivity of the conical surface of the concentrator/reflector.
- ε_{upp} : emissivity of the upper surface of the autoclave.

The radiosities $J_{\text{lat}}, J_{\text{upp}}$, and J_{ref} are calculated using the following equations :

$$J_{\text{lat}} = \varepsilon_{\text{lat}} \sigma T_{\text{lat}}^4 + (1-\varepsilon_{\text{lat}})\left(J_{\text{ref}} F_{\text{lat-ref}} + J_{\text{ape}} F_{\text{lat-ape}}\right) \tag{3.33}$$

$$J_{\text{ref}} = \varepsilon_{\text{ref}} \sigma T_{\text{ref}}^4 + (1-\varepsilon_{\text{ref}})\left(J_{\text{lat}} F_{\text{ref-lat}} + J_{\text{ref}} F_{\text{ref-ref}} + J_{\text{lat}} F_{\text{ref-lat}}\right) \tag{3.34}$$

$$J_{\text{ape}} = \varepsilon_{\text{ref}}\sigma T_{\text{ref}}^4 + 0 = \varepsilon_{\text{env}}\sigma T_{\text{env}}^4 \tag{3.35}$$

The shape factor $F_{\text{lat-ref}}$ is :

$$F_{\text{lat-ref}} = \frac{1}{2\pi}\left[\cos^{-1}\frac{B}{A} - \frac{1}{2y}\left(\sqrt{((A+2)^2 - 4x^2)}\cos^{-1}\frac{B}{xA} + B\sin^{-1}\frac{1}{x} - \frac{\pi A}{2}\right)\right] \tag{3.36}$$

where :

$$x = \frac{R_{\text{ape}}}{R_{\text{aut}}} \tag{3.37}$$

We can also calculate the ratio :

$$y = \frac{L}{R_{\text{aut}}} \tag{3.38}$$

- L : Length of the autoclave
- R_{ape} : Radius of the conical aperture
- R_{aut} : Radius of the autoclave

$$\begin{aligned} A &= x^2 + y^2 - 1 \\ B &= y^2 - x^2 + 1 \end{aligned} \tag{3.39}$$

For surfaces oriented normal to solar rays, the shape factors are :

$$\begin{aligned} F_{\text{app-gro}} &= \frac{1}{2}\left[1 - \sin(h_s)\right] \\ F_{\text{app-sky}} &= \frac{1}{2}\left[1 + \sin(h_s)\right] \end{aligned} \tag{3.40}$$

Where :

$F_{\text{uoo-gro}}$: Shape factor of the upper surface of the autoclave to the ground

$F_{\text{uoo-sky}}$: Shape factor of the upper surface of the autoclave to the sky

The emissivity ε_a of the atmospheric air is given by :

$$\varepsilon_{\text{air}} = 1 - 0.261e^{-7.77\times10^{-4}T_{\text{env}}^2} \tag{3.41}$$

$$\begin{aligned}(m_{\text{water}}c_{\text{water}} + m_{\text{aut}}c_{\text{aut}})\frac{dT_{\text{aut}}(t)}{dt} &= I_N A_{\text{ape}}\rho_{\text{ref}}\alpha_{\text{lat}} \\ &\quad - [h_{\text{lat}}A_{\text{lat}}(T_{\text{lat}} - T_{\text{env}}) \\ &\quad + h_{\text{upp}}A_{\text{upp}}(T_{\text{upp}} - T_{\text{env}}) \\ &\quad + \frac{A_{\text{lat}}\varepsilon_{\text{lat}}}{1-\varepsilon_{\text{lat}}}\left(\sigma T_{\text{lat}}^4 - J_{\text{lat}}\right) \\ &\quad + \frac{A_{\text{upp}}\varepsilon_{\text{upp}}}{1-\varepsilon_{\text{upp}}}\left(\sigma T_{\text{upp}}^4 - J_{\text{upp}}\right)]\end{aligned} \tag{3.42}$$

Where :

- σ : Stefan-Boltzmann constant, 5.67×10^{-8} W/m$^2 \cdot$ K^4
- m_{water} : Mass of the water in the autoclave
- m_{aut} : Mass of the autoclave
- c_{water} : Specific heat capacity of water
- c_{aut} : Specific heat capacity of the autoclave
- $T_{\text{aut}}(t)$: Temperature of the autoclave as a function of time, obtained by solving the equation using a numerical method (4th order Runge-Kutta)
- I_N : Solar irradiance normal to the aperture area
- A_{ape} : Aperture area of the solar concentrator
- ρ_{ref} : Reflectivity of the concentrator
- α_{lat} : Absorptivity of the lateral surface
- h_{lat} : Convection heat transfer coefficient of the lateral surface
- A_{lat} : Area of the lateral surface
- T_{lat} : Temperature of the lateral surface
- h_{upp} : Convection heat transfer coefficient of the upper surface

- A_{upp} : Area of the upper surface
- T_{upp} : Temperature of the upper surface
- T_{env} : Ambient temperature
- ε_{lat} : Emissivity of the lateral surface
- J_{lat} : Radiosity of the lateral surface
- ε_{upp} : Emissivity of the upper surface
- J_{upp} : Radiosity of the upper surface

the value of T_{aut} being obtained by solving the equation by a numerical method (Range-Kutta of order 4). the autoclave fluid temperature defined as :

$$T_{\text{water}} = \frac{T_{\text{aut}} + T_{\text{env}}}{2} \tag{3.43}$$

3.9 Thermal Efficiency of the Solar Autoclave

The thermal efficiency η_{th} of the solar autoclave is given by :

$$\eta_{\text{th}} = F_R \eta_o - \left(\frac{F_R U_L}{C_R}\right) \frac{T_{\text{lat}} - T_{\text{env}}}{I_N} \tag{3.44}$$

where :

$$\eta_o = \rho_{\text{ref}} \alpha_{\text{lat}} = 0.9 \times 0.95 = 0.855\,(85.5\%) \tag{3.45}$$

The heat removal factor F_R is defined as :

$$F_R = \frac{mc_{\text{water}}}{A_{\text{lat}} U_L} \left[1 - \exp\left(-\frac{A_{\text{lat}} U_L F'}{\dot{m} c_{\text{water}}}\right)\right] \tag{3.46}$$

where

F' **:** Collector efficiency factor

U_L **:** Overall heat loss coefficient from the autoclave

m **:** Mass of the water

$\dot{m}$ **:** Mass flow rate of water

The overall heat loss coefficient from the autoclave, U_L, is given by :

$$U_L = \frac{Q_{\text{los}}}{A_{\text{aut}} \left(T_{\text{aut}} - T_{\text{env}}\right)} \tag{3.47}$$

Clapeyron's equation describes the evolution of the pressure of the saturated steam of the water in the autoclave as a function of the change in its temperature :

$$p_{\text{sat}} = p_0 \exp\left[\frac{M \cdot L_v}{R}\left(\frac{1}{T_0} - \frac{1}{T_{\text{water}}}\right)\right] \tag{3.48}$$

Where :

- T_0 : Boiling temperature of the water at a given pressure p_0, in K.
- p_{sat} : Saturated vapor pressure, in the same unit as p_0.
- M : Molar mass of the water, in kg/mol, for water $M = 0.018\,\text{kg/mol}$.
- L_v : Latent heat of vaporization of the substance, in J/kg, $L_v = 2.26 \times 10^6\,\text{J/kg}$ (at 100°C).
- R : Ideal gas constant, equal to $8.31\,\text{J}\,\text{mol}^{-1}\,\text{K}^{-1}$; T : Steam temperature, in K.

3.10 Computer program for simulation

We have developed a computational code in Fortran language, which can provide early knowledge about temperature distribution, solar irradiation and temperature at the receiver/autoclave. The Runge-Kutta algorithm of order 4 allows the solution of the partial differential equation.Figures 3.2 and 3.3 shows the following flowchart, which presents the procedure for calculating the evolution of the temperature of the autoclave and what it contains, as well as the saturating pressure produced by heating the water.

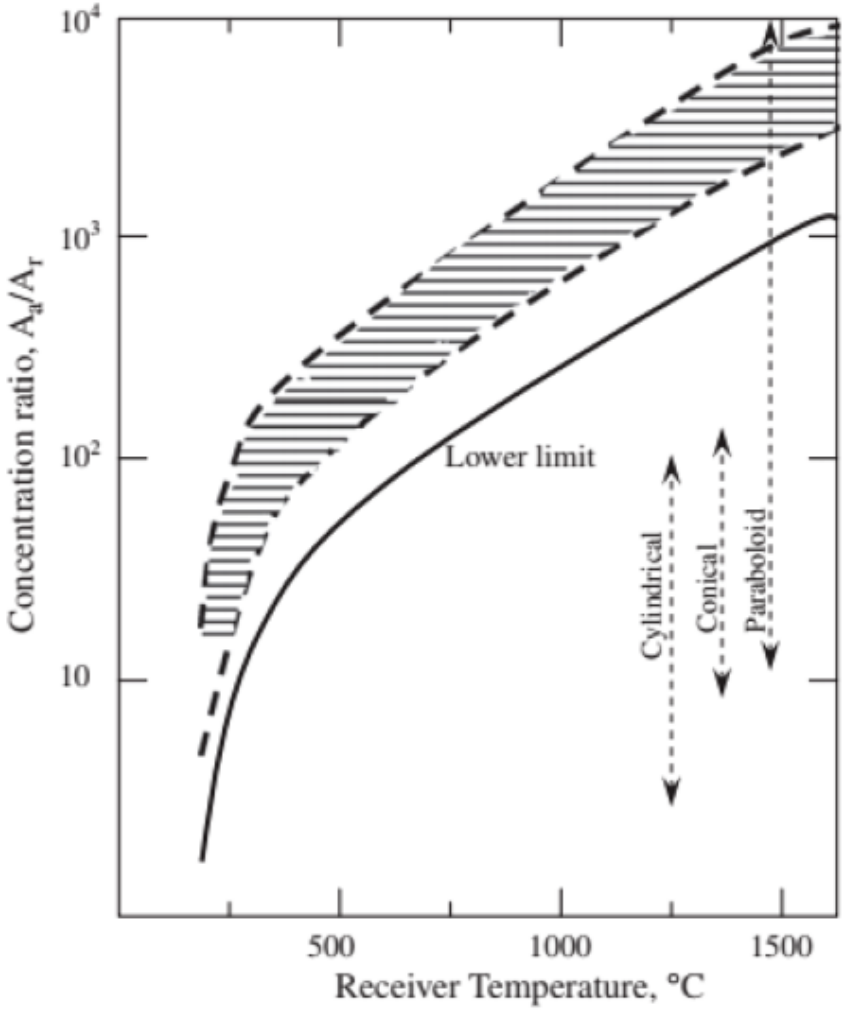

FIGURE 3.2 : Curves of concentration ratio C_R as a function of receiver temperature for different geometric shapes of reflector.

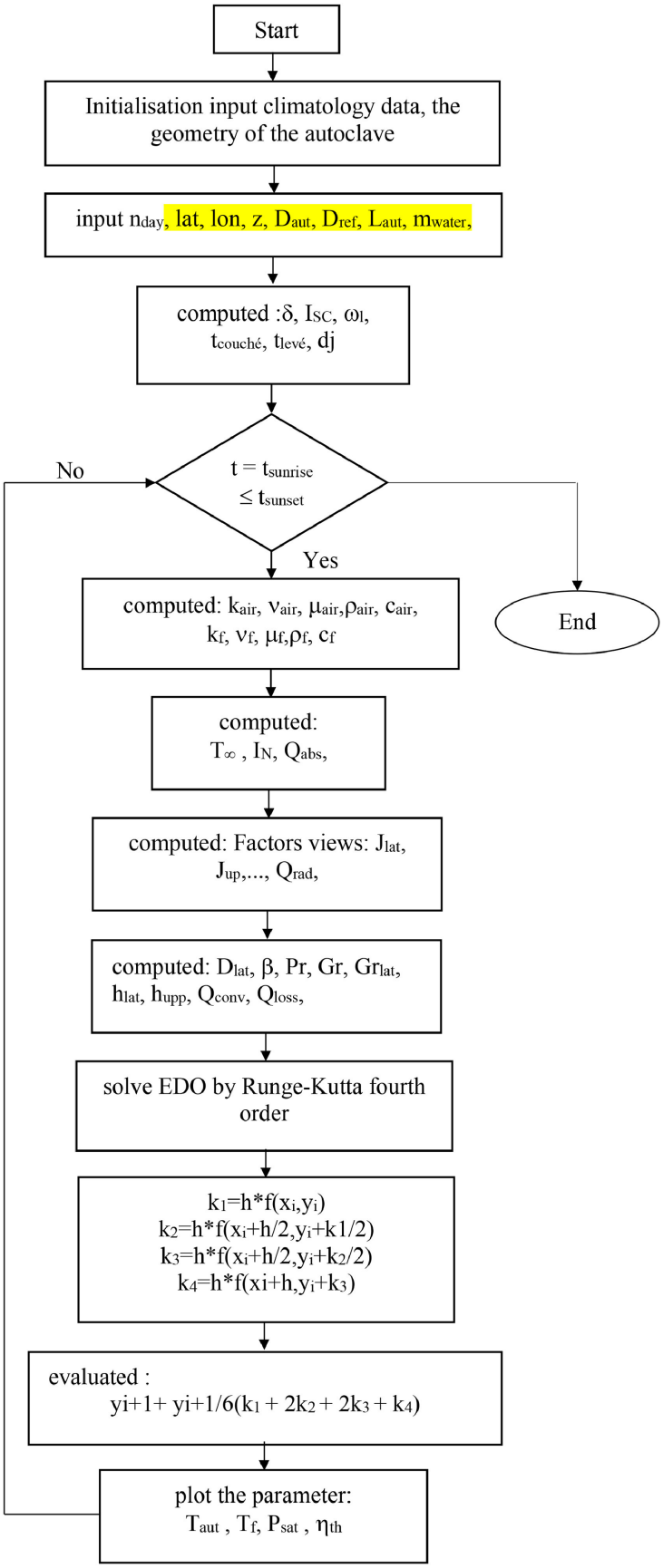

FIGURE 3.3 : Flowchart for calculating physical parameters.

Chapitre 4

Results and Interpretation

4.1 Simulation Results

In this part, the modelling results are presented. In all cases, the fluid's initial temperature and the environment were defined, and other parameters according to winter and summer, such as heating temperature, average autoclave temperature and thermal losses, were calculated.Figure 4.1 shows that the concentration ratio decreases as the diameter of the conical concentrator autoclave increases.

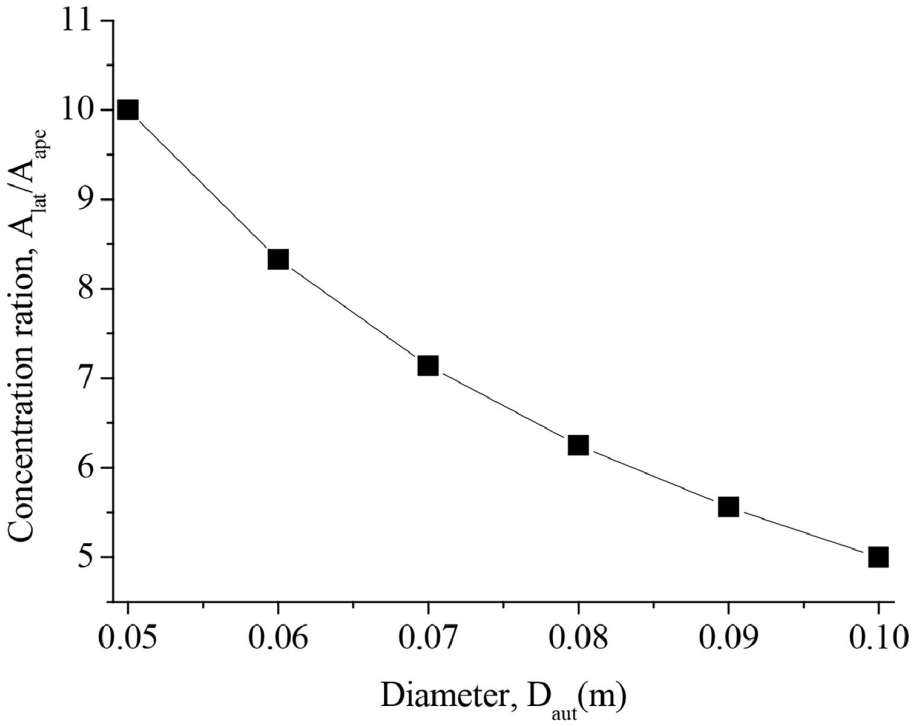

FIGURE 4.1 : variation of concentration ratio with variation of autoclave diameter.

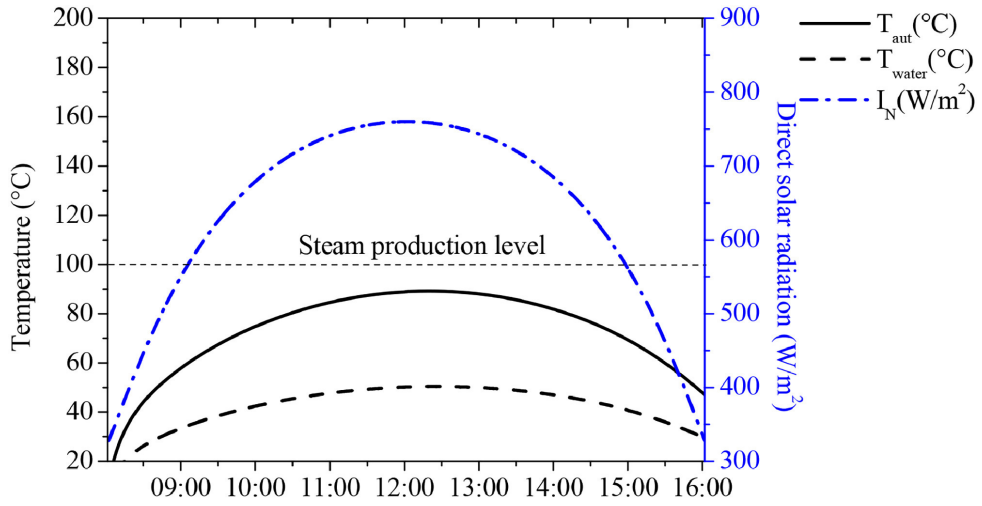

FIGURE 4.2 : Hourly variation of autoclave temperature (T_{aut}), ambient temperature (T_{env}), and direct normal solar radiation (I_{N}) for 21 December (m = 0.9 kg, D_{aut} = 0.10 m)

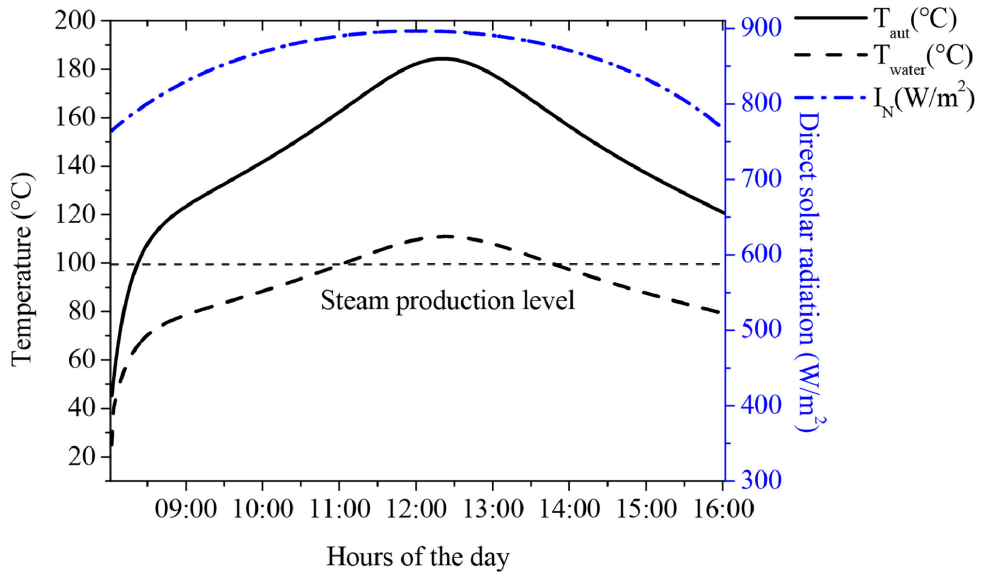

FIGURE 4.3 : Hourly variation of autoclave temperature (T_{aut}), ambient temperature (T_{env}), and direct normal solar radiation (I_{N}) for 21 June ($m = 0.9$ kg, $D_{\text{aut}} = 0.10$ m).

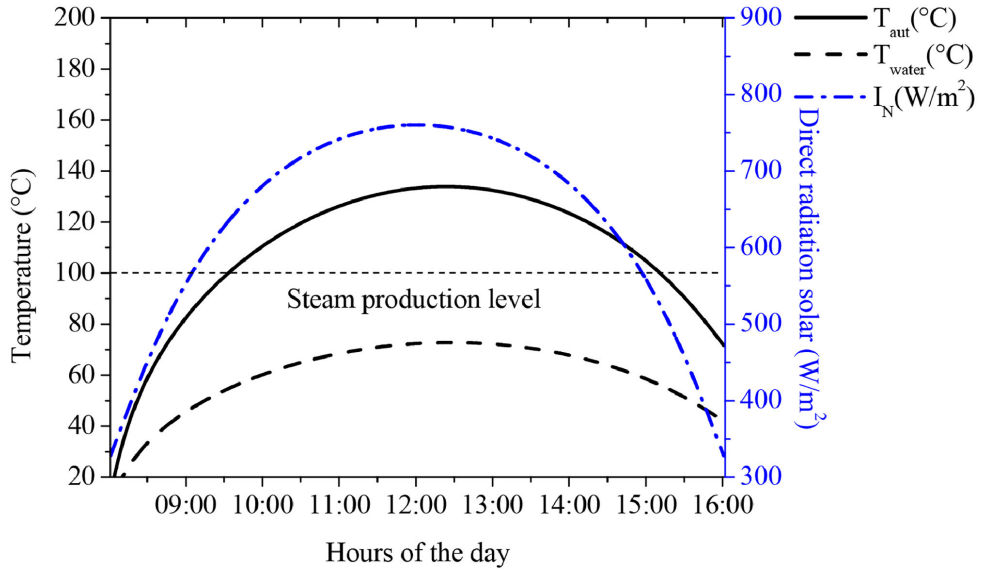

FIGURE 4.4 : Hourly variation of autoclave temperature (T_{aut}), ambient temperature (T_{env}), and direct normal solar radiation (I_{N}) for 21 December (m = 0.9 kg, D_{aut} = 0.05 m)

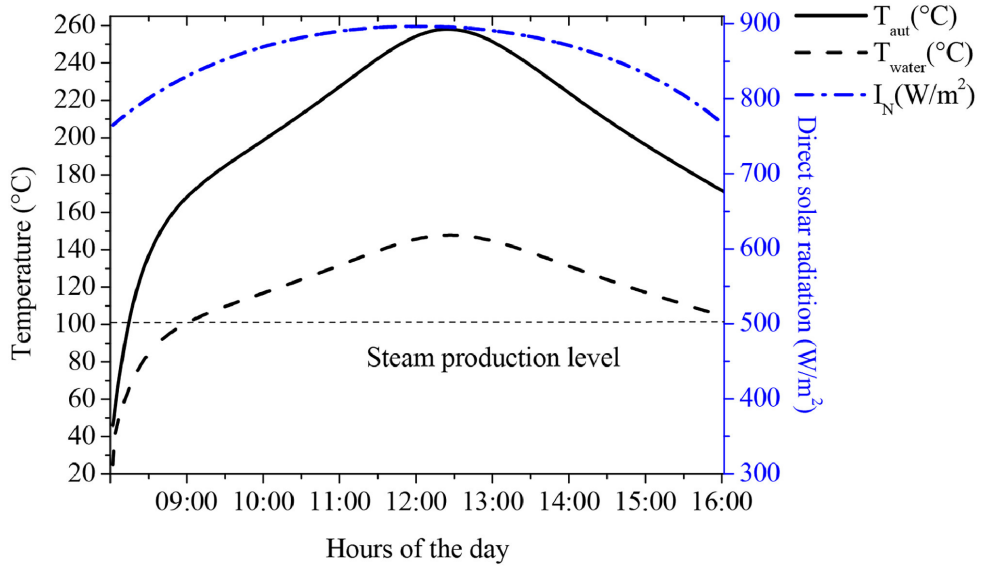

FIGURE 4.5 : Hourly variation of autoclave temperature (T_{aut}), ambient temperature (T_{env}), and direct normal solar radiation (I_{N}) for 21 June ($m = 0.9$ kg, $D_{\text{aut}} = 0.05$ m)

The following Fig.4.6 shows the influence of the diameter of the autoclave on the water temperature ; the reduction in the diameter of the autoclave causes an increase in the geometric concentration, which therefore increases the temperature at the autoclave level. A sizeable geometric concentration, therefore, a large concentrated flow on the side surface of the autoclave increases the temperature value to high levels.

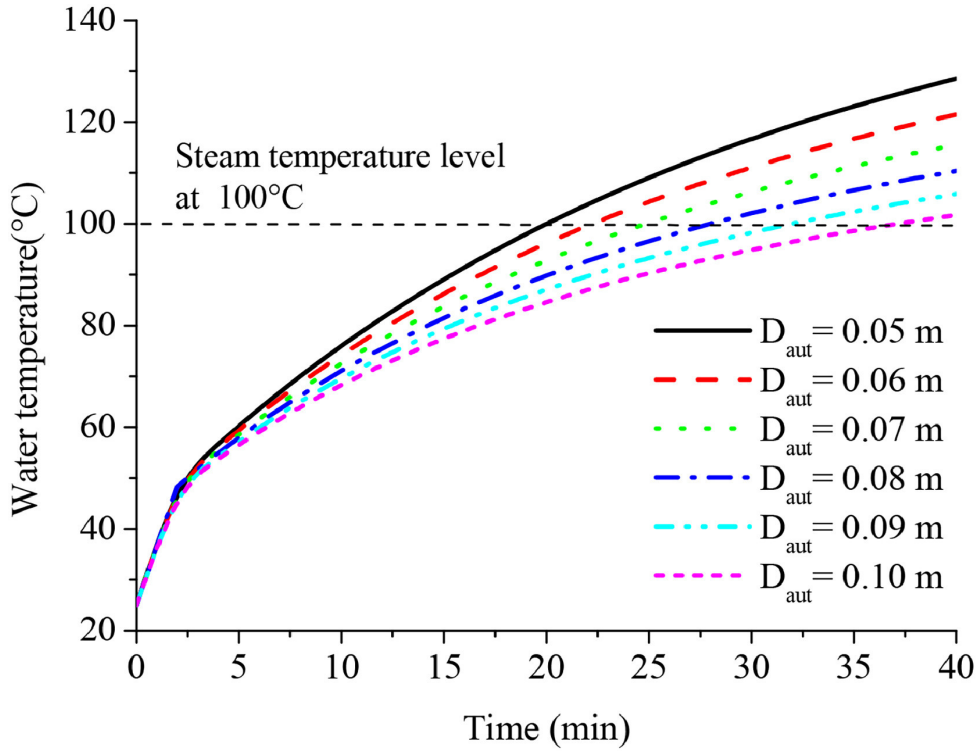

FIGURE 4.6 : Influence of the autoclave diameter

This modeling approach was validated by comparing the mathematical model with Bahadori's numerical results from 1976. The temperature distribution of the autoclave in March was compared with data measured by Bahadori, as shown in Figure 4.7. A strong agreement was observed between the numerical and measured data, with statistically significant results, including a very high R-squared value (greater than 0.980) and a low P-value. In Figure 4.7, the increase in wind speed is seen to increase heat losses, which in turn reduces the temperature of the autoclave. The use of the solar autoclave for water heating and the production of saturated steam with stationary fluid inside the autoclave is not highly effective due to the stagnation temperature reached after a short time in summer and, to a lesser extent, in winter. The efficiency of the conical concentrator drops to zero after a certain heating period, making it necessary to change the contents of the autoclave, leading to the conclusion that this type of model cannot be used continuously throughout the day. We can define the stagnation temperature as the point when the thermal efficiency of the autoclave reaches zero, according to Equation(4.1).

$$T_{\text{stag}} = \frac{C_R \rho_{\text{ref}} \alpha_{\text{lat}} I_N}{U_L} + T_{\text{env}} \tag{4.1}$$

The parameter presented is the thermal efficiency of the solar

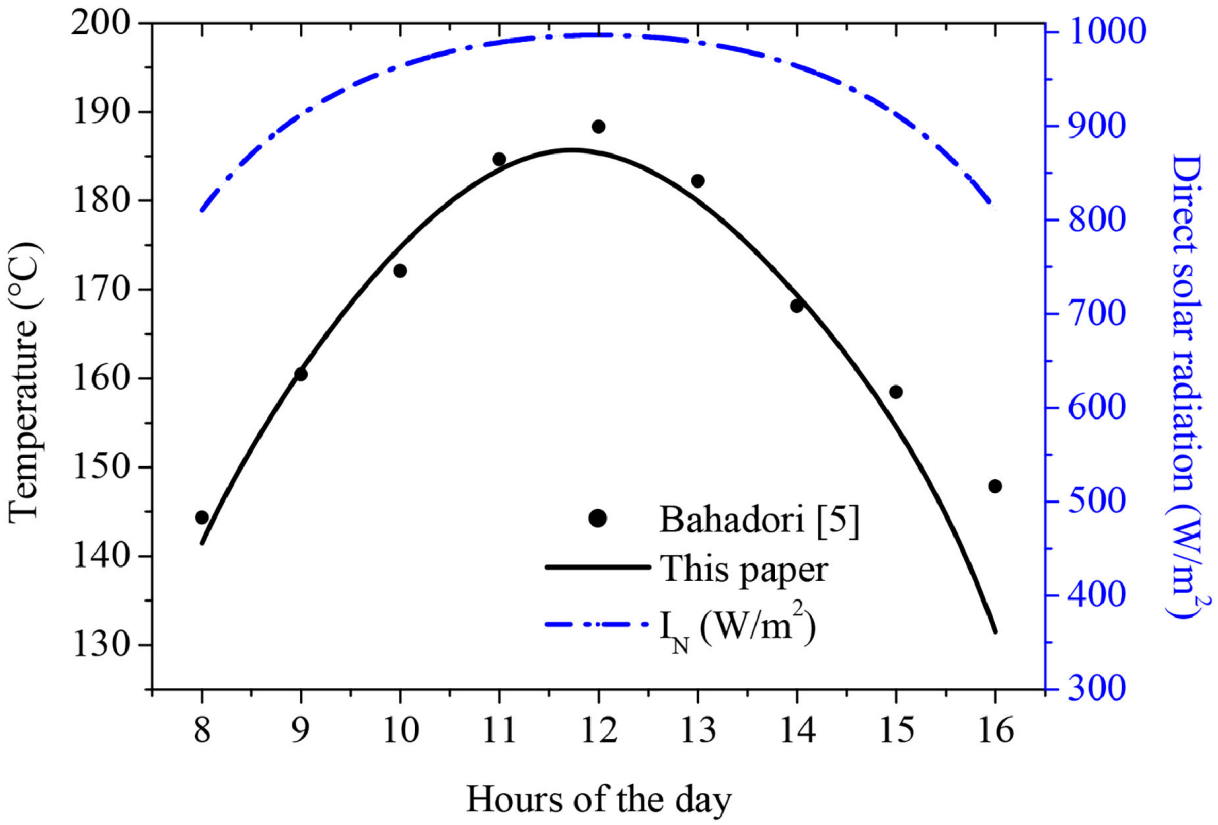

FIGURE 4.7 : Comparison of mathematical model results and Bahadori's data (1976, $m = 0.9$ kg, $D_{\text{aut}} = 0.05$ m) for 21 June.

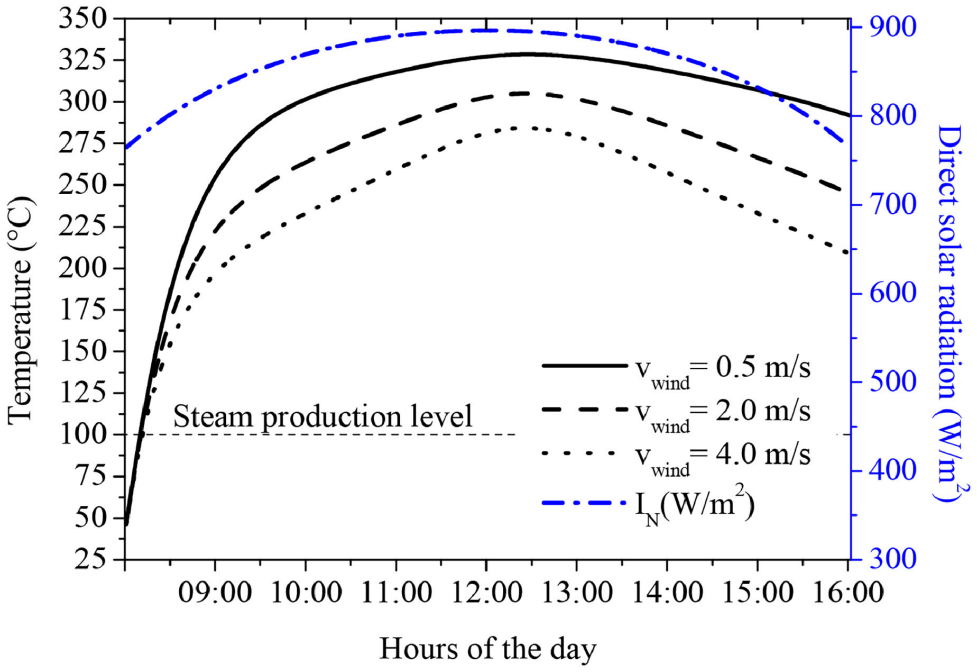

FIGURE 4.8 : Influence of wind on autoclave temperature for 21 June (m = 0.9 kg, D_{aut} = 0.05 m).

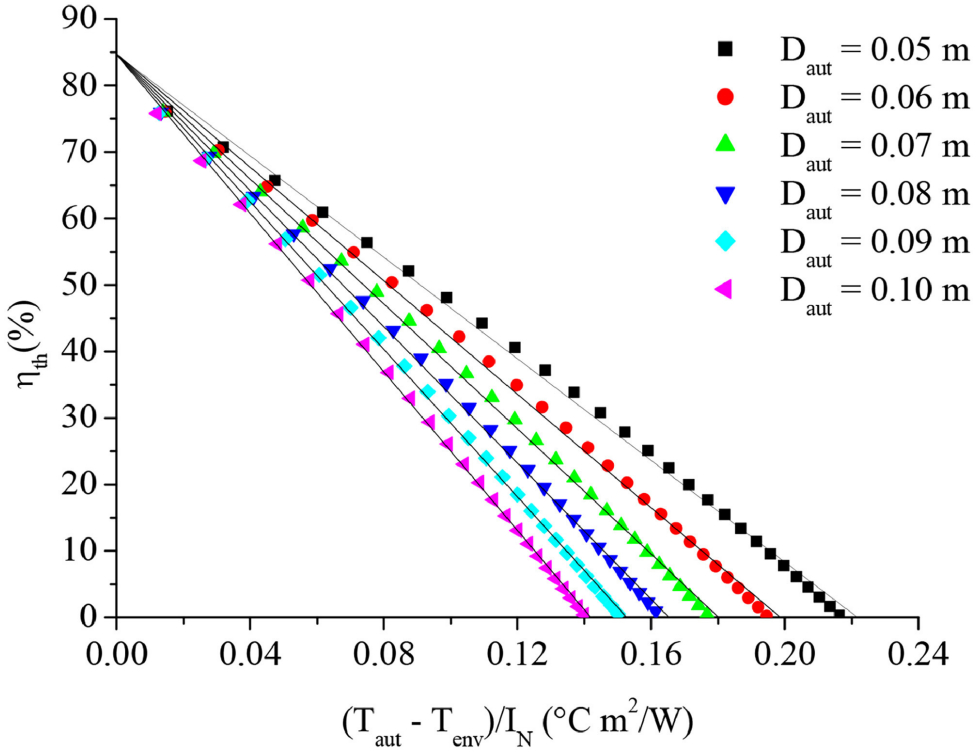

FIGURE 4.9 : Thermal efficiency curve for different diameters of the solar autoclave (m_{water} = 0.3 kg).

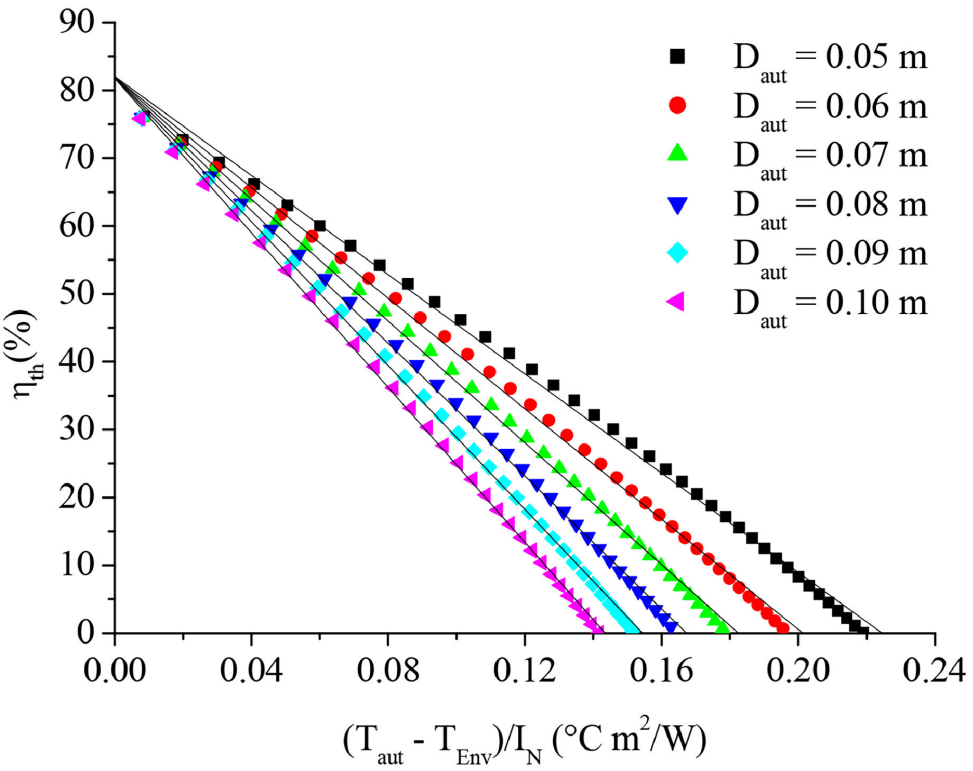

FIGURE 4.10 : Thermal efficiency curve for different diameters of the solar autoclave ($m_{\text{water}} = 0.6$ kg).

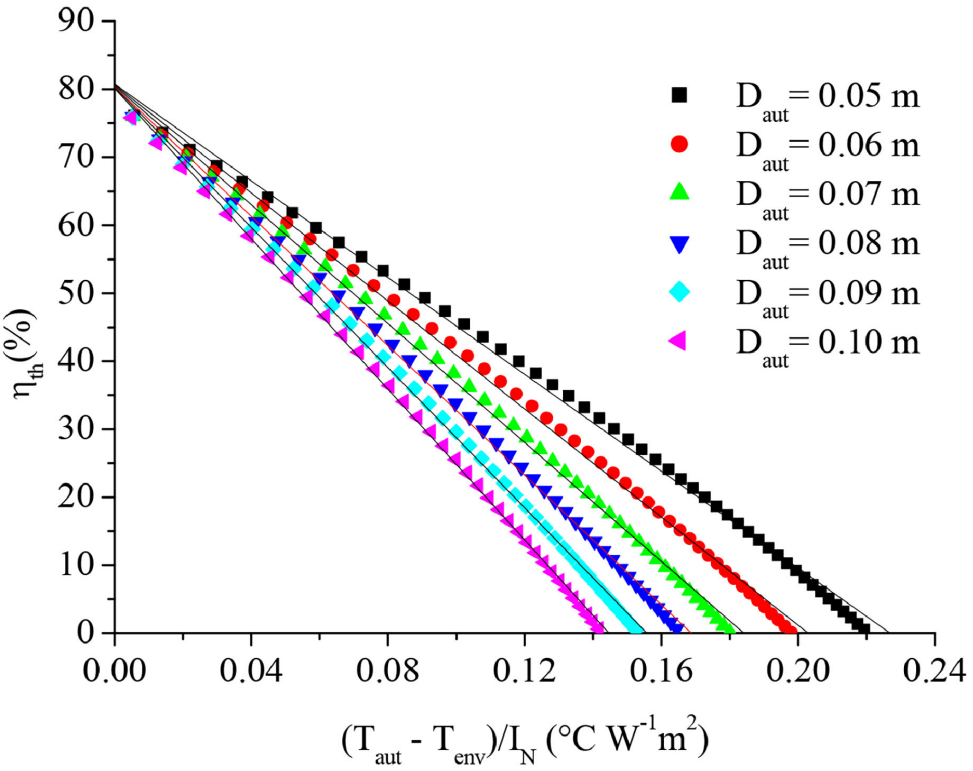

FIGURE 4.11 : Thermal efficiency curve for different diameters of the solar autoclave ($m_{\text{water}} = 0.9$ kg).

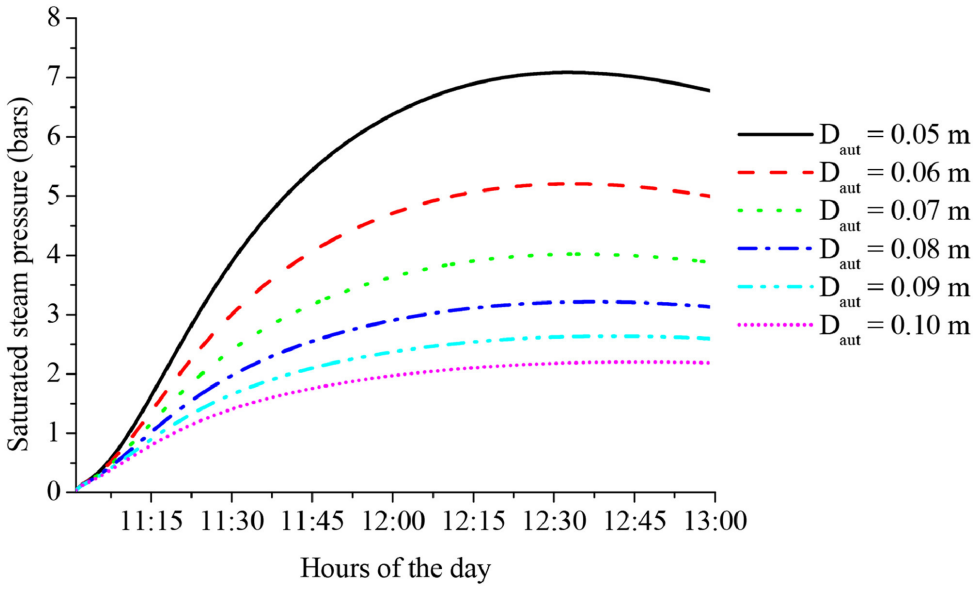

FIGURE 4.12 : Variation of pressure as a function of diameter for $m = 0.3$ kg on 21 June.

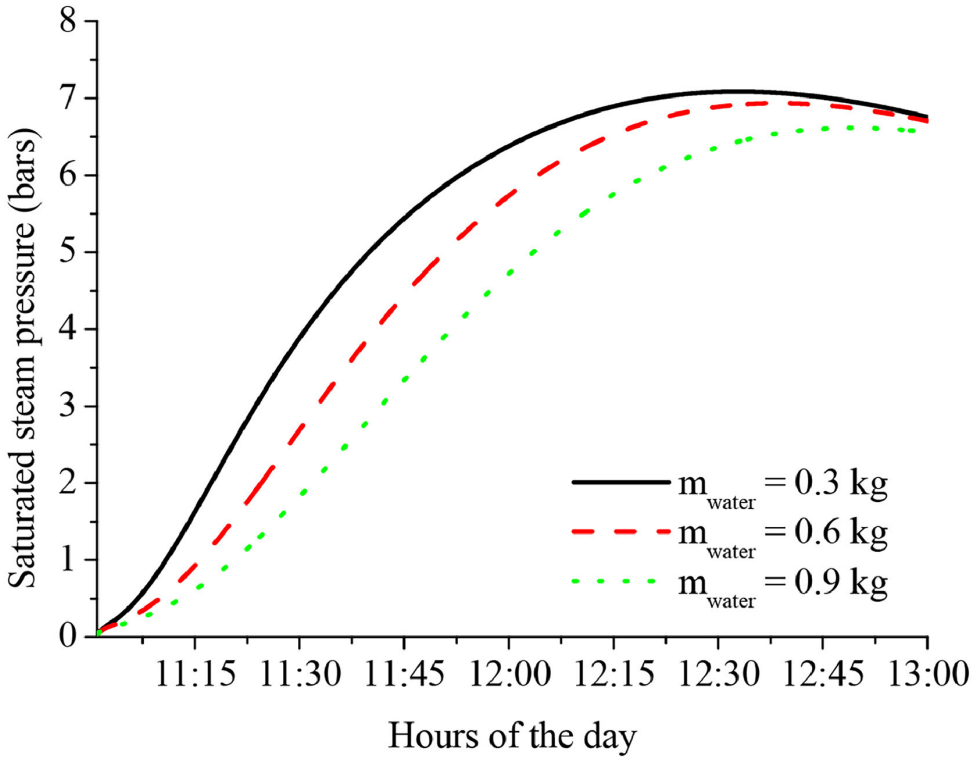

FIGURE 4.13 : Variation of pressure as a function of water mass for $D_{\text{aut}} = 0.05$ m on 21 June.

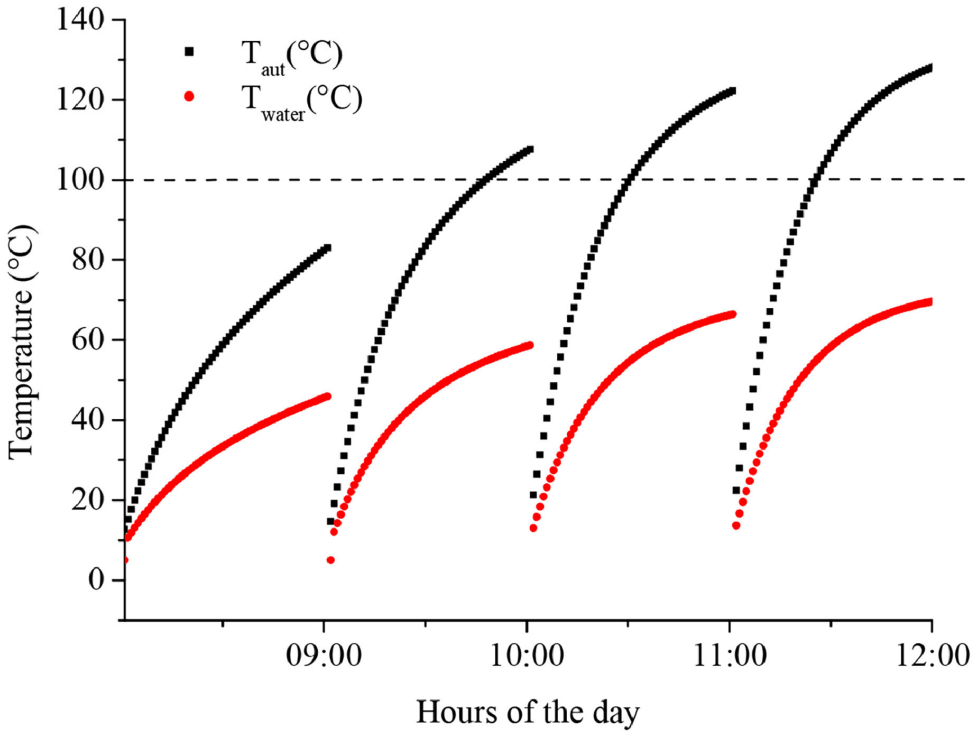

FIGURE 4.14 : Duration of heating of the autoclave water during the different hours of the day on December 21.

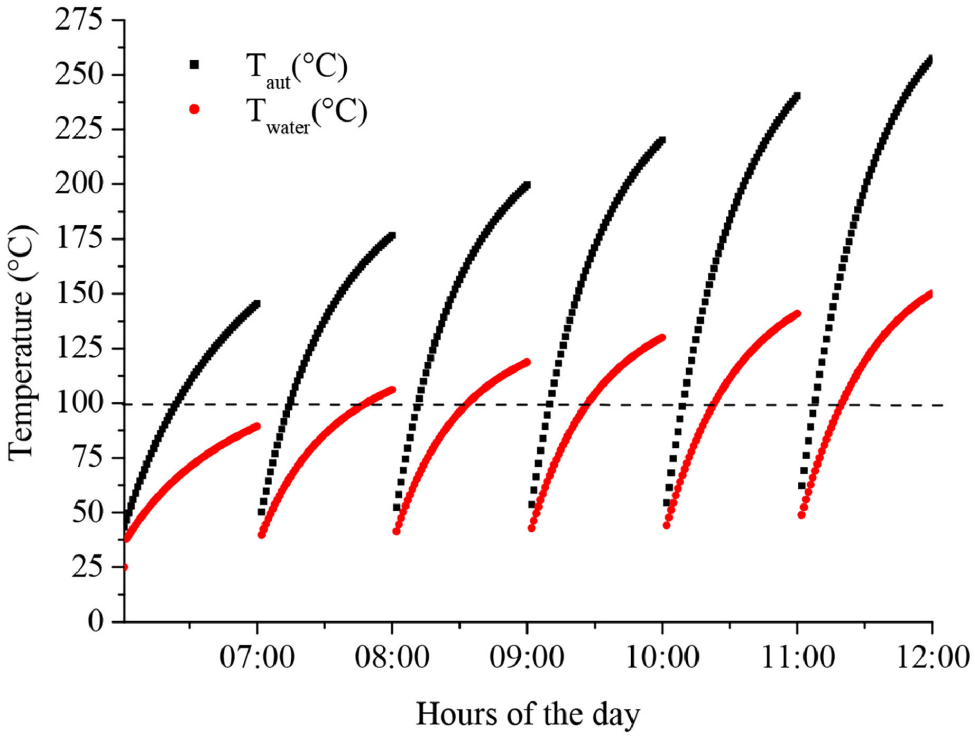

FIGURE 4.15 : Duration of heating of the autoclave water during the different hours of the day of June 21.

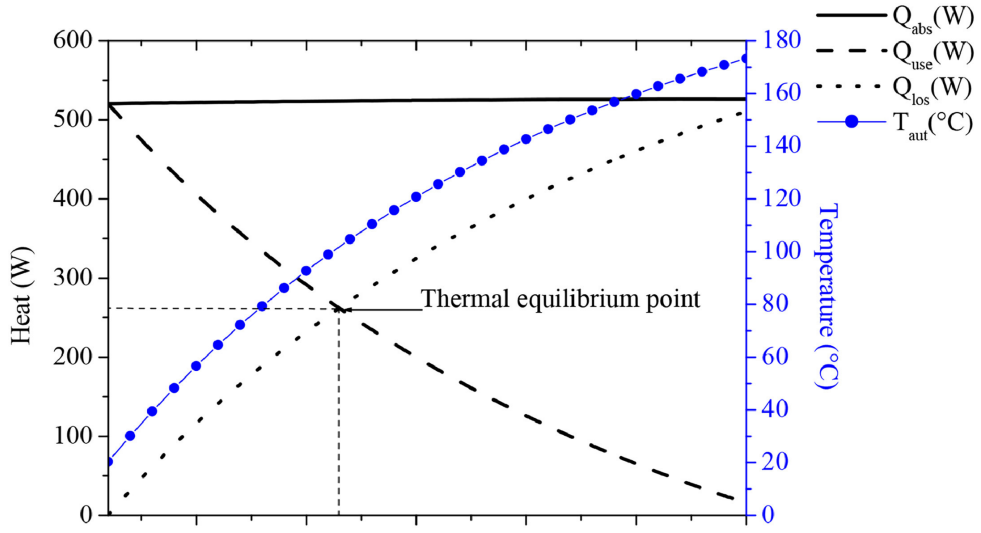

FIGURE 4.16 : Graph of simulation that began at 11 :00 h solar time on December 21, with $I_N = 878.6$ W/m^2, $D_{\text{aut}} = 0.05$ m, $C_R \approx 10$, and $m_{\text{water}} = 0.6$ kg.

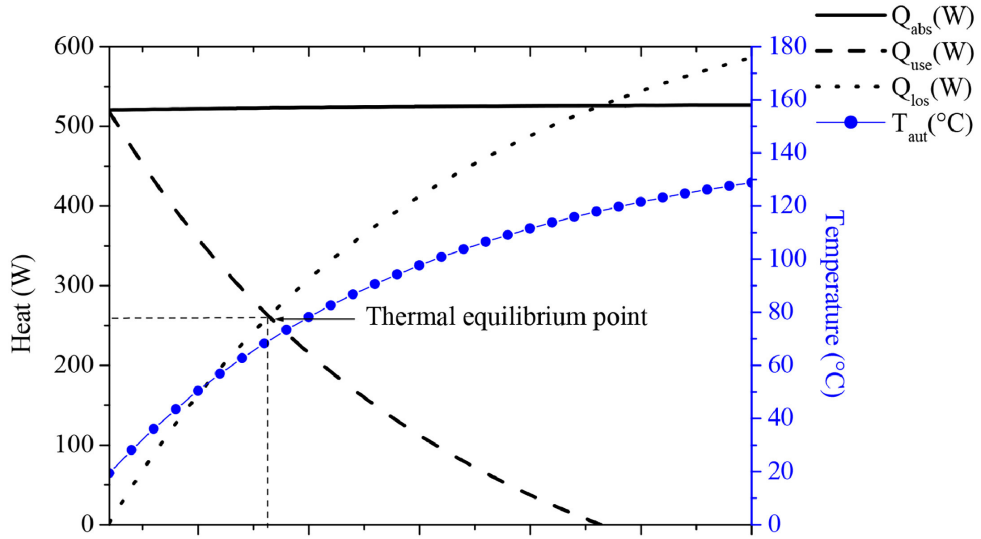

FIGURE 4.17 : Graph of simulation that began at 11 :00 h solar time on December 21, with $I_N = 878.6$ W/m^2, $D_{\text{aut}} = 0.1$ m, $C_R \approx 5$, and $m_{\text{water}} = 0.6$ kg.

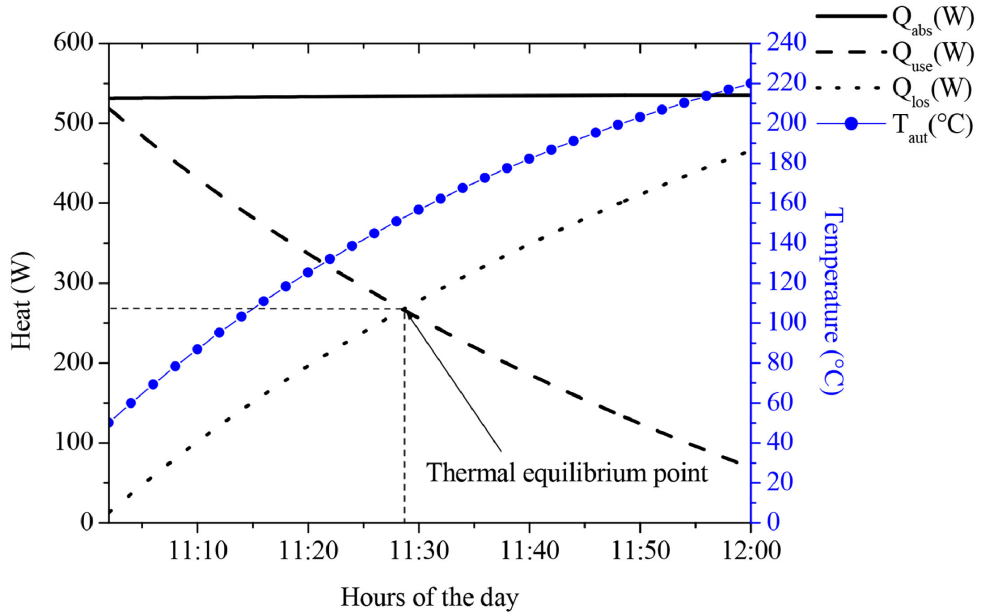

FIGURE 4.18 : Graph of simulation that began at 11 :00 h solar time on June 21, with $I_N = 894.5$ W/m^2, $D_{\text{aut}} = 0.05$ m, $C_R \approx 10$, and $m_{\text{water}} = 0.6$ kg.

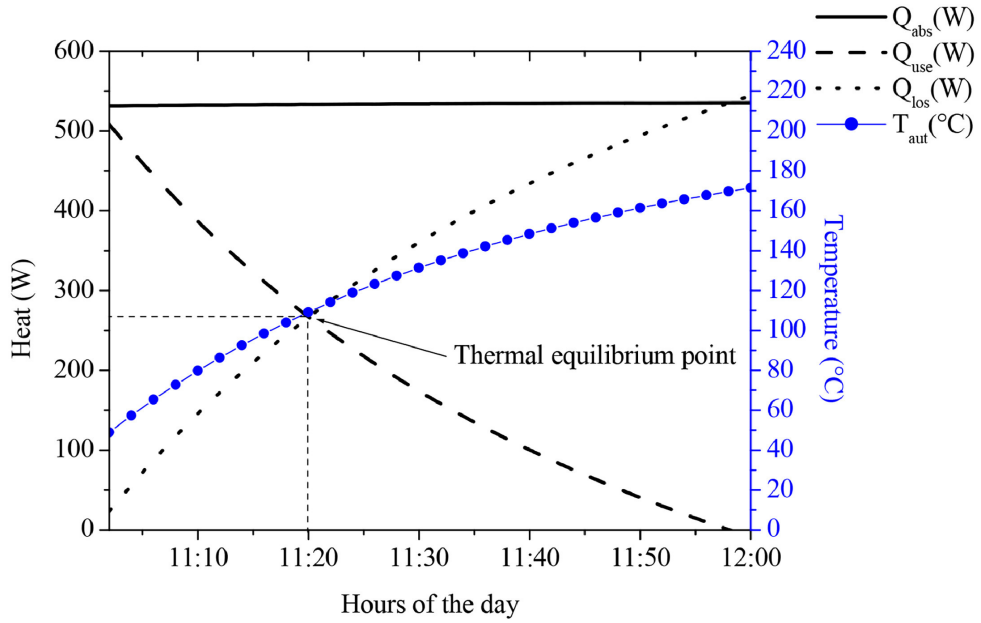

FIGURE 4.19 : Graph of simulation that began at 11 :00 h solar time on June 21, with $I_N = 894.5$ W/m^2, $D_{\text{aut}} = 0.1$ m, $C_R \approx 5$, and $m_{\text{water}} = 0.6$ kg.

TABLE 4.1 : Parameters of the investigated configurations

Parameters	**Symbol**	**Value**
Lateral surface of the absorber	A_{lat} (m^2)	$3.1415e-1$
Upper surface of the autoclave	A_{upp} (m^2)	$3.1415e-2$
Lower surface of the autoclave	A_{low} (m^2)	$3.1415e-2$
Aperture surface of the cone	A_{apr} (m^2)	1.1309
Reflector surface of the cone	A_{ref} (m^2)	1.4721
Autoclave Length	L (m)	0.5
Concentration factor	C_R	$A_{\text{apr}}/A_{\text{lat}}$
Emissivity	$\epsilon_{\text{lat}} = \epsilon_{\text{upp}} = \epsilon_{\text{ref}}$	0.95
Atmospheric emissivity	ϵ_{atm}	~ 0.7
Ground emissivity	ϵ_{gro}	0.9
Reflector reflectivity	ρ_{ref}	0.8
Ground reflectivity	ρ_{gro}	0.2

TABLE 4.2 : Main results : F_R and U_L for different receiver tube diameters (0.3 kg)

Coefficients	$D = 0.05$	$D = 0.06$	$D = 0.07$	$D = 0.08$	$D = 0.09$	$D = 0.10$
C_R	10	8.33	7.14	6.25	5.56	5
$\text{F}_\text{R}\eta_\text{O}$	0.846	0.847	0.847	0.846	0.846	0.846
F_R	0.996	0.997	0.996	0.996	0.996	0.995
$\text{F}_\text{R}\text{U}_\text{L}/\text{C}_\text{R}(\%)$	3.816	4.265	4.698	5.119	5.546	5.964
U_L ($\text{W/m}^2\,^\circ\text{C}$)	38.30	35.63	33.65	32.12	30.95	29.94
T_stag ($^\circ$C)	239.3	219.6	203.3	189.4	179.1	169.9

TABLE 4.3 : Main results : F_R and U_L for different receiver tube diameters (0.6 kg)

Coefficients	$D = 0.05$	$D = 0.06$	$D = 0.07$	$D = 0.08$	$D = 0.09$	$D = 0.10$
C_R	10	8.33	7.14	6.25	5.56	5
$\text{F}_\text{R}\eta_\text{O}(\%)$	82.063	81.931	81.888	81.822	81.839	81.801
F_R	0.965	0.963	0.963	0.962	0.962	0.962
$\text{F}_\text{R}\text{U}_\text{L}/\text{C}_\text{R}(\%)$	3.654	4.070	4.485	4.889	5.299	5.698
U_L ($\text{W/m}^2\,^\circ\text{C}$)	37.85	35.18	33.24	31.74	30.60	29.60
T_stag ($^\circ$C)	241.67	220.45	204.51	190.84	180.69	171.73

TABLE 4.4 : Main results : F_R and U_L for different receiver tube diameters (0.9 kg).

Coefficients	$D = 0.05$	$D = 0.06$	$D = 0.07$	$D = 0.08$	$D = 0.09$	$D = 0.10$
C_R	10	8.33	7.14	6.25	5.56	5
$F_R\eta_O(\%)$	80.766	80.651	80.520	80.373	80.292	80.200
F_R	0.950	0.948	0.947	0.945	0.944	0.943
$F_R U_L/C_R(\%)$	3.56	3.97	4.37	4.76	5.16	5.54
U_L (W/m^2 K)	37.463	34.891	32.972	31.487	30.344	29.366
T_{stag} (°C)	241.97	222.64	206.42	192.39	181.51	171.83

$$\text{For } D_{\text{aut}} = 0.09\,\text{m}: \quad \eta_{\text{th}}(\%) = 84.6 - 5.546\left(\frac{T_{\text{aut}} - T_{\text{env}}}{I_N}\right) \tag{4.2}$$

$$\text{For } D_{\text{aut}} = 0.10\,\text{m}: \quad \eta_{\text{th}}(\%) = 84.6 - 5.964\left(\frac{T_{\text{aut}} - T_{\text{env}}}{I_N}\right) \tag{4.3}$$

Equations that describe the thermal efficiency of the solar autoclave for different diameters are given as follows :

$$\text{For } D_{\text{aut}} = 0.05\,\text{m}: \quad \eta_{\text{th}}(\%) = 82.063 - 3.654\left(\frac{T_{\text{aut}} - T_{\text{env}}}{I_N}\right) \tag{4.4}$$

$$\text{For } D_{\text{aut}} = 0.06\,\text{m}: \quad \eta_{\text{th}}(\%) = 81.931 - 4.070\left(\frac{T_{\text{aut}} - T_{\text{env}}}{I_N}\right) \tag{4.5}$$

$$\text{For } D_{\text{aut}} = 0.07\,\text{m}: \quad \eta_{\text{th}}(\%) = 81.888 - 4.485\left(\frac{T_{\text{aut}} - T_{\text{env}}}{I_N}\right) \tag{4.6}$$

$$\text{For } D_{\text{aut}} = 0.08\,\text{m}: \quad \eta_{\text{th}}(\%) = 81.822 - 4.889\left(\frac{T_{\text{aut}} - T_{\text{env}}}{I_N}\right) \tag{4.7}$$

$$\text{For } D_{\text{aut}} = 0.09\,\text{m}: \quad \eta_{\text{th}}(\%) = 81.839 - 5.299\left(\frac{T_{\text{aut}} - T_{\text{env}}}{I_N}\right) \tag{4.8}$$

$$\text{For } D_{\text{aut}} = 0.10\,\text{m}: \quad \eta_{\text{th}}(\%) = 81.801 - 5.698\left(\frac{T_{\text{aut}} - T_{\text{env}}}{I_N}\right) \tag{4.9}$$

Equations that describe the thermal efficiency of the solar autoclave for different diameters are given as follows :

$$\text{For } D_{\text{aut}} = 0.05\,\text{m}: \quad \eta_{\text{th}}(\%) = 80.766 - 3.559\left(\frac{T_{\text{aut}} - T_{\text{env}}}{I_N}\right) \tag{4.10}$$

$$\text{For } D_{\text{aut}} = 0.06\,\text{m}: \quad \eta_{\text{th}}(\%) = 81.931 - 4.070\left(\frac{T_{\text{aut}} - T_{\text{env}}}{I_N}\right) \tag{4.11}$$

$$\text{For } D_{\text{aut}} = 0.07\,\text{m}: \quad \eta_{\text{th}}(\%) = 81.888 - 4.485\left(\frac{T_{\text{aut}} - T_{\text{env}}}{I_N}\right) \tag{4.12}$$

$$\text{For } D_{\text{aut}} = 0.08\,\text{m}: \quad \eta_{\text{th}}(\%) = 81.822 - 4.889\left(\frac{T_{\text{aut}} - T_{\text{env}}}{I_N}\right) \tag{4.13}$$

$$\text{For } D_{\text{aut}} = 0.9\,\text{m}: \quad \eta_{\text{th}}(\%) = 81.839 - 5.299\left(\frac{T_{\text{aut}} - T_{\text{env}}}{I_N}\right) \tag{4.14}$$

$$\text{For } D_{\text{aut}} = 0.10\,\text{m}: \quad \eta_{\text{th}}(\%) = 81.801 - 5.698\left(\frac{T_{\text{aut}} - T_{\text{env}}}{I_N}\right) \tag{4.15}$$

4.2 Analysis of Results

This coefficient is relatively high due to the absence of coverage and the significant convection losses. The thermal convection coefficient is approximately $10\,\text{W/m}^2\,^\circ\text{C}$, so the total heat loss coefficient is higher than this value, ranging from approximately 29.36 to $38.30\,\text{W/m}^2\,^\circ\text{C}$. These high values are acceptable as they include radiation losses. It was observed that the thermal efficiency is at its maximum when the temperature of the autoclave matches the temperature of the environment. This condition occurs only at the beginning of each heating operation. As the temperature increases, the thermal efficiency of the autoclave decreases. The efficiency of the autoclave significantly decreases as the diameters increase because the autoclave transfers a large portion of the heat to the external environment due to the increased lateral surface, which explains the decreased

concentration ratio C_R. Additionally, there is no variation in the shape of the curves when altering the quantity of water.

Figure 4.12 illustrates the impact of the autoclave diameter on the pressure of the saturated steam. An increase in the autoclave diameter results in a decrease in pressure, which consequently reduces the temperature within the autoclave. An increase in geometric concentration leads to a higher concentrated flow on the side surface of the autoclave, which raises the temperature to higher levels and increases the steam pressure. Figure 4.13 shows that increasing the mass of water added to the autoclave results in a rise in steam production and pressure by several additional bars.

Figures 4.14 and 4.15 depict the variation in the temperature of the autoclave and the water over two specific days (December 21 and June 21). The temperature increases over time in all operations. After each cooling period, the temperature of the autoclave and the water equalizes with the ambient temperature. Differences in autoclave temperature between winter and summer are attributed to solar radiation intensity. It is also noted that the heating speed in summer is over three times faster compared to winter Figures 4.5 and 4.11.

Figures 4.16 , 4.17 , 4.18 and 4.19 illustrate the evolution of heat losses and the heat used and absorbed during heating on December 21 for two different diameters of the autoclave ($D_{\text{aut}} = 0.05\,\text{m}$ and $0.10\,\text{m}$). It is observed that the heat absorbed by the side surface of the autoclave is lower than the heat received by the conical opening of the reflector. This variation is due to losses from reflection and absorption by the conical reflector and the autoclave Figures 4.3 , 4.4.

As the temperature of the side surface of the autoclave increases, heat is transferred to the environment through conduction, radiation, and convection. The greater the temperature difference between the absorber and the ambient air, the higher the heat losses from the conical concentrator and the lower the useful heat. Heating continues until thermal equilibrium is achieved between useful heat and waste heat, i.e., at 11 :22 a.m. for $D_{\text{aut}} = 0.05\,\text{m}$ and 11 :16 a.m. for $D_{\text{aut}} = 0.10\,\text{m}$ in winter, and at 11 :28 a.m. for $D_{\text{aut}} = 0.05\,\text{m}$ and 11 :20 a.m. for $D_{\text{aut}} = 0.10\,\text{m}$ in summer. At this point, equilibrium temperature is reached Figures 4.16 , 4.2-4.5 , 4.11 and Table 1–1 to 1-4 .

4.3 Chapter Conclusion

In this chapter, we developed and analyzed a mathematical model for the evolution of water temperature in an autoclave powered by solar energy through a conical reflector. The model's validity was established through comparisons with published literature, demonstrating its capability to accurately describe physical phenomena. Specifically, it successfully identifies the phase change point near 100 °C, marking the onset of phase transition within the thermodynamic system. The model also indicates that a concentration ratio around 10 is effective for steam production under moderate radiation conditions. It estimates that the time required to generate saturating steam and achieve pressures of approximately 7 bars for a diameter of 0.05 m is feasible under standard conditions. Overall, the mathematical model has proven effective in predicting the temperature dynamics of the autoclave and the water. The insights gained from this model pave the way for proposed modifications to enhance the system's performance and efficiency.

General conclusion

This study has addressed a significant challenge in the field of medical sterilization, particularly in low-resource settings where traditional sterilization methods are often impractical or infeasible. The development of a solar-powered autoclave presents a promising solution to improve healthcare outcomes by ensuring effective sterilization of medical equipment in environments with limited access to conventional energy sources.

Our research involved a comprehensive approach to designing and optimizing a solar autoclave, integrating a conical solar concentrator with an autoclave system to utilize solar energy for generating the necessary steam. Through the creation of a detailed mathematical model, we have accurately predicted the thermal behavior of water within the autoclave, demonstrating that it can achieve the requisite temperatures for effective sterilization. The results indicate that our system can produce saturated steam and reach temperatures exceeding 121°C within 20 to 30 minutes, depending on environmental conditions and the dimensions of the autoclave.

The successful validation of our model against literature results underscores the robustness of our design. The solar autoclave's ability to consistently achieve and maintain the critical sterilization temperatures provides a reliable alternative to conventional methods, particularly in developing regions where energy access is a persistent challenge. Our findings highlight the potential for solar energy to serve as a cost-effective and sustainable solution for medical sterilization, contributing to the reduction of healthcare-associated infections (HAIs) and improving overall healthcare quality.

The research presented in this thesis is structured to provide a thorough understanding of the components and functionality of the solar autoclave. Chapter One offers a detailed exploration of traditional autoclave technology, laying the foundation for understanding the evolution and need for alternative sterilization methods. Chapter Two delves into solar collectors, examining their role in harnessing solar energy and their integration into the autoclave system. Chapter Three focuses on the numerical study and optimization of the conical autoclave receiver, providing insights into the design parameters and performance

metrics. Finally, Chapter Four presents the results of our research, demonstrating the efficacy of the solar autoclave and its potential impact on healthcare practices.

Future research should aim to further refine the solar autoclave design to enhance its performance and adaptability across various operational environments. Investigations into the long-term reliability and maintenance of the system, as well as its scalability for different healthcare settings, will be essential for broader implementation. Additionally, exploring the integration of advanced materials and technologies could improve the efficiency and sustainability of the solar autoclave.

In conclusion, this study contributes valuable knowledge to the field of renewable energy applications in medical sterilization. By leveraging solar energy, we offer a practical and innovative solution that addresses the dual challenges of energy access and infection control. This research not only advances the understanding of solar autoclave systems but also paves the way for future developments in sustainable healthcare technologies.

This work highlights the importance of interdisciplinary approaches in tackling global health challenges and underscores the potential of renewable energy solutions in transforming medical practices. As we move forward, continued innovation and research will be crucial in ensuring that such technologies can be effectively implemented and scaled to meet the needs of healthcare systems worldwide.

Bibliographie

[1] World Health Organization, *Decontamination and Reprocessing of Medical Devices for Health-Care Facilities* (World Health Organization, Geneva, 2016).

[2] S. Trabia, Honors College Theses (2012).

[3] K. Mahdi, K. Bekrentchir, N. Bellel et S. Boulaaras, Partial Differential Equations in Applied Mathematics **10**, 100659 (2024).

[4] O. Sadjere, American Journal of Sciences and Engineering Research (2020).

[5] C. M. Technologies, website celitron (06-07-2021).

[6] S. A. S. Alkadhim, SSRN Electronic Journal, 10.2139/ssrn.3340320 (2018).

[7] N. Andrews, The History of the Autoclave (2022).

[8] M. T. Mustapha, D. Uzun Ozsahin, B. Uzun et I. Ozsahin, in *Applications of Multi-Criteria Decision-Making Theories in Healthcare and Biomedical Engineering*, sous la dir. d'I. Ozsahin, D. U. Ozsahin et B. Uzun (Academic Press, 2021), p. 197-216.

[9] P. Sonawwanay et V. Raja, International Journal of Ambient Energy **39**, 1 (2017).

[10] I. Chinelo, International Journal of Basic and Applied Sciences **3**, 490 (2014).

[11] M. N. Bahadori, Solar Energy **18**, 489 (1976).

[12] M. Tyroller, *SOLAR STEAM STERILIZER FOR RURAL HOSPITALS*, 2006.

[13] D. A. Schuler, T. Kaseman et J. Boubour, The American Journal of Tropical Medicine and Hygiene **87**, 602 (2012).

[14] M. Dravid, A. Chandak, S. Phute, R. Khadse, H. Adchitre et S. Kulkarni, Journal of Hospital Infection **80**, 345 (2012).

[15] O. Neumann, C. Feronti, A. D. Neumann, A. Dong, K. Schell, B. Lu, E. Kim, M. Quinn, S. Thompson, N. Grady, P. Nordlander, M. Oden et N. J. Halas, Proceedings of the National Academy of Sciences **110**, 11677 (2013).

[16] B. Lawrence, E. Brettner, Y. Liu, K. Godwin et A. Compton, Northern Arizona University (2013).

[17] D. L. Chandler, Massachusetts Institute of Technology (FEBRUARY 26, 2013).

[18] B. Sadhana, L. Prasad et G. Satyanand, International Journal of Emerging Technology and Advanced Engineering **4**, 203 (2014).

[19] R. Buxbaum, Duke University Certificate in Energy and Environment 2014 - 2015 (2015).

[20] N. K. Sharma, Department of Mechanical Engineering, SRM University, Sonipat,- 131029, Haryana,, India, I. K. Sharma, Department of Mechanical Engineering, SRM University, Sonipat,- 131029, Haryana,, India, L. Sharma, Department of Commerce, Lakshmi Bai College, University of Delhi-110024, Delhi, India, P. Rajgopal et Department of Commerce, Lakshmi Bai College, University of Delhi-110024, Delhi, India, Indian Journal of Science and Technology **10**, 1 (2017).

[21] A. V. T. Sajan Thomas, H. M. Akash Pillai et G. M, International Journal for Innovative Research in Science and Technology (april 2017).

[22] A. Haileslasie, A. Abrha et E. Minas, Momona Ethiopian Journal of Science **10**, 163 (2019).

[23] H. Birhanu et M. B. Kahsay, INTERNATIONAL JOURNAL OF ADVANCED RESEARCH IN ENGINEERING & TECHNOLOGY **9**, 293 (2018).

[24] X. Wang, Y. Liu, R. Feng, Y. Zhang, C. Chang, B. Fu, T. Luan, P. Tao, W. Shang, J. Wu, C. Song et T. Deng, Progress in Natural Science: Materials International **29**, 10 (2019).

[25] B. B. Lin Zhao, *Solar-powered device sterilizes medical equipment*, Physics World, (16 déc. 2020) https://physicsworld.com/a/solar-powered-device-sterilizes-medical-equipment/.

[26] M. K. Yadav, A. Modi et S. B. Kedare, Springer Singapore (2020).